Title

THREE-DIMENSIONAL RECONSTRUCTION OF SOLENOIDAL AND IRROTATIONAL COMPONENTS OF TENSOR FIELDS

Authors

Gullberg, Grant
Defrise, Michael
Panin, Vladimir
et al.

Publication Date

2022-02-08

Peer reviewed

Revised 8/23/2000

THREE-DIMENSIONAL RECONSTRUCTION OF SOLENOIDAL AND IRROTATIONAL COMPONENTS OF TENSOR FIELDS

Grant T. Gullberg and Michel Defrise

Vrije University Brussels, Belgium

Vladimir Panin and Gengsheng L. Zeng

University of Utah

Technical Report LBNL- 2001448
Lawrence Berkeley National Laboratory
February 8, 2022

ABSTRACT

Tensor tomography is being investigated as a technique for reconstruction of *in vivo* tensor fields that can be used to develop more accurate models of the properties of biological tissue. This paper presents filter backprojection algorithms for reconstructing 3D second order tensor fields from either 3D planar or 3D line measurements. A Helmhotz-type of decomposition is proposed for tensor fields. Using this decomposition, a Fourier projection theorem is formulated in terms of the solenoidal and irrotational components of the tensor field. From this, it is shown that the solenoidal component of the tensor field can be reconstructed from either a single set of X-ray directional measurements or a combination of X-ray and Radon directional measurements. Also, from the Fourier projection theorem, a set of Radon directional measurements that will reconstruct the solenoidal and irrotational components of the tensor field is prescribed. This means that for the X-ray transform we only need to measure the scalar product of the tensor field with the unit vector along the projection ray. For the 3D Radon transform, this corresponds to measuring plane integrals of the scalar product with the vector orthogonal to the plane. Based on these observations filtered backprojection reconstruction formulas are prescribed for the reconstruction of 3D tensor fields from X-ray and Radon measurements. Results of computer simulations that demonstrate the validity of the mathematical formulations are presented.

INTRODUCTION

There is an increasing need to measure *in vivo* tensor quantities (diffusion, strain, stress, and conductivity) for the purpose of developing more accurate models of the properties of biological tissue in order to improve diagnosis of various diseases. MRI has already been demonstrated to have the capacity to image brain [1], cardiac diffusion tensor fields [2]-[5], and cardiac strain-rate tensor fields [6]-[8]. In particular, the diffusion-tensor MRI may eventually be useful in characterizing myocardial fiber structure [2]-[5]. Knowledge of fiber bundle orientation will be useful for specifying material axes of a mechanical model [9]-[14] and for identifying conductive pathways for electrical models of the heart [15]. We point out that all of this work uses non-tomographic techniques to measure diffusion and strain tensor fields. However, it may be advantageous to use MRI tensor tomography, which has the potential to allow fast imaging and provide images that are immune to motion artifacts. The aim of this paper is to develop general three-dimensional inversion formulae for computed tomography of tensor fields. The motivation behind this work is to determine if these reconstruction techniques may help in the ultimate goal of determining whether, for specific applications, tensor tomography could provide a more accurate and a more efficient method of measuring tensor fields than the more direct techniques that have already been developed in MRI.

First, we must make it clear that tensor tomography is not necessary for obtaining 3D mappings of tensor fields. MRI is unique in that it does not require computed tomography to form a three-dimensional image of internal structures. However, recently there has been much interest in using projection reconstruction techniques for various MRI applications because projection reconstruction techniques are useful for processing data that is acquired rapidly, which can be used to follow dynamic processes and can be less sensitive to motion artifacts. Of recent interest is the use of projection reconstruction techniques to image diffusion tensor fields [16]. The tomographic method that is used is quite different than the method that we are discussing in this paper. Diffusion weighted images are obtained from projection reconstruction techniques. From the reconstructed diffusion weighted images the tensor fields are calculated using standard methods of a combination of various gradient weighted reconstructed images [17], [18]. The

method we propose differs in that scalar projections of the diffusion tensor field are obtained at several projections and the diffusion tensor field, instead of diffusion weighted images, is reconstructed directly from these projections.

This brings us to an important **second** point. At present, there is no known method to form scalar projection measurements of tensor fields without performing some approximation [19]. That is, there is no existing tensor detector. We point out that in our method, to form projections of diffusion tensor fields, MRI approximations had to be made [19]. At the present there is no known technique, using MRI, which will form projections of either vector [20] or tensor fields [19] without this approximation. A past problem in the application of vector field tomography was the formation of scalar projections for arbitrary probe directions. Either approximations were made, as in the application of MRI [20], or techniques did not exist to measure all of the necessary components of the vector field, as in ultrasound time of flight measurements. For this application, only the component of the vector field projected (longitudinal measurements) onto the line of integration could be measured [21].

First, to understand the history of the development of vector and tensor field tomography one must understand the **Helmholtz decomposition** of a vector field. The Helmholtz decomposition states that if the source and circulation components of a vector field vanish at infinity, a vector field can be written as the sum of a solenoidal component (divergence-free, also referred to as source-free component) and an irrotational component (curl-free component) [22]. The solenoidal component can be expressed as the curl of a vector potential ($\nabla\times\Psi$) and the irrotational component can be expressed as the gradient of a scalar potential ($\nabla\Phi$). In our discussion to follow, one will appreciate the importance of the Helmholtz decomposition in understanding the relationships between which projection measurements will reconstruct solenoidal components of the vector field and which projection measurements will reconstruct irrotational components of the vector field.

Tensor tomography builds on much of the work that has already been accomplished in **vector field tomography** [20], [21], [23]-[48]. An excellent review of this work is given by Sparr and Strahlen [48]. Several of the applications have involved acoustic flow imaging using

time-of-flight measurements - ultrasonic imaging in medicine [21], acoustic flow imaging in nondestructive evaluation [23], and ocean acoustic tomography [24], [25]. One of the earlier studies was performed by Johnson *et al.* [21] who used ultrasound to reconstruct velocity vector fields in blood vessels from acoustic time-of-flight measurements. The projection measurements were the integral of the projected component of the velocity vector field onto the line forming the projection measurement (also called the longitudinal projection measurement [32]). Johnson *et al*. [21] used an iterative algebraic reconstruction algorithm (ART) to compute what was later understood by Norton [26], [27] to be the divergence-free component of the vector field fulfilling homogeneous Neumann boundary conditions (i.e., the normal component of the divergence-free component at the boundary is zero). Using the Helmholtz decomposition and the Fourier central-slice theorem, Norton [26], [27] derived a reconstruction method for the velocity field and showed that the reconstruction of the acoustic time-of-flight (longitudinal projection) measurements with boundary conditions allows reconstruction of a divergence-free vector field composed of a solenoidal component that satisfies homogeneous boundary conditions and an irrotational component defined by the gradient on the boundary. It was shown that the longitudinal measurements alone could not recover the irrotational component of the vector field. Additional information in terms of boundary conditions were needed to reconstruct the irrotational component of a divergence free vector field.

Before Norton's important contribution, Kramer and Lauterbur [28] developed a hybrid filtered backprojection algorithm for the reconstruction of flow using NMR. They showed that some flow components could not be reconstructed from the longitudinal projection measurements. Working independently, Winters and Rouseff [29] also developed a Fourier central section theorem for the reconstruction of the divergence-free component, which they argued was important for specifying the vorticity of fluid flow [29], [30], [31].

Later Braun and Hauck [32] showed (not using Fourier projection techniques but spatial convolution techniques) that projection of the orthogonal component of the velocity vector field (the transverse projection measurement, which is the integral of the orthogonal component of the velocity vector field along the line of the projection measurement) allows one to reconstruct the

irrotational component of the vector field. This irrotational (curl-free) component along with the divergence-free (solenoidal) component gives the complete determination of the flow vector field. Braun and Hauck [32] recognized that bounded domains admit harmonic vector fields that are both irrotational and solenoidal. Therefore, the decomposition into irrotational and solenoidal components is not unique. In their paper, they proposed that the decomposition should be $V = V^S_{\Psi_S} + V^I_{\Phi_I} + V_H$, where $V^S_{\Psi_S} = \nabla \times \Psi_S$, $V^I_{\Phi_I} = \nabla \Phi_I$, and V_H is the harmonic component of the vector field satisfying $\nabla^T V_H = 0$ and $\nabla \times V_H = 0$. The solenoidal component $V^S_{\Psi_S}$ is homogeneous in the sense that the normal component of $V^S_{\Psi_S}$ is zero on the boundary and is totally tangential to the boundary. The curl-free component $V^I_{\Phi_I}$ is homogenous in the sense that the tangential component of $V^I_{\Phi_I}$ vanishes on the boundary and is exactly normal to the boundary.

Later, Prince [20] extended the previous work in 2D to 3D by developing filtered backprojection algorithms that could be used to reconstruct both the solenoidal and irrotational components of the vector field from 3D Radon projections. Prince generalized the longitudinal and transverse measurements of Braun and Hauck [32] by defining a more general inner product measurement (probe transform) which forms an inner product between the vector field and a unit-vector probe direction. Prince [20] showed that in 3D only one set of probe measurements (the irrotational measurements) is required to reconstruct the irrotational component and that two sets of probe measurements (the solenoidal measurements) are required to reconstruct the solenoidal component. The three probe directions form a linearly independent set of vectors. (The study by Prince [20] is particularly noteworthy because it defines the principles from which methods can be developed for measuring projections of diffusion tensors using MRI.) Sparr [48] took this further and showed that the vector ray transform (in our work we refer to this as the vector X-ray transform) can recover the solenoidal component of the vector field and the vector Radon normal transform can recover the irrotational component of the vector field. However,

these results need to be studied further because it is not clear what type of angular sampling is necessary to recover the solenoidal component. The question remains whether it is necessary to sample the entire unit sphere, or whether one great circle sampling is sufficient, or if sampling over multiple great circles is required to reconstruct the solenoidal component?

Norton [26] - [27], and Braun and Hauck [32], and later Osman and Prince [33] were all concerned about the vector tomography problem on bounded domains. In fact, physical problems are often defined on bounded domains and it is the boundary that creates or partially defines the field. Braun and Hauck [32] considered the 2D problem on a circular domain and later Osman and Prince [33] extended this to a general 3D domain. Braun and Hauck [32] showed that the harmonic component is reconstructed equally between the irrotational and solenoidal measurements. Whereas, Osman and Prince [33] showed that the harmonic component of a 3D vector field is not imaged equally in the irrotational and solenoidal measurements. In fact Osman and Prince [33] characterized the homogenous component as V_{Ξ}^{H} where $V_{\Xi}^{H}=-\nabla\Xi$ for some harmonic function Ξ satisfying Laplace's equation $\nabla^2\Xi=0$ on the domain. The work of Osman and Prince [33] considered only the Radon transform. They showed that the irrotational measurements could be used to reconstruct both the irrotational component, which has homogeneous boundary conditions, and the harmonic component that arises from the normal field component on the boundary. By solving the Poisson equation $\nabla^2\Phi_I=\nabla^2\Phi$ ($\Phi=\Phi_I+\Phi_H$ is known from the irrotational field reconstruction) with the Dirchlet boundary conditions $\Phi_I=C$, one can separate the homogeneous and harmonic components of the irrotational component. Similarly, the solenoidal measurements can be used to reconstruct both the solenoidal component, which has homogeneous boundary conditions, and the harmonic component that arises from the tangential field component on the boundary. By solving $\nabla\times\nabla\times\Psi_S=\nabla\times\nabla\times\Psi$ ($\Psi=\Psi_S+\Psi_H$ is known from the solenoidal field reconstruction) with the solenoidal boundary conditions ($\nabla\times\Psi$ is tangential on the boundary), one can

separate homogeneous and harmonic components.

Works of vector tomography have been applied in other applications such as; optics, to measure flow [26], [27]; deflection optical tomography, to determine densities in supersonic expansions and flames [34]; optical tensor field tomography in a Kerr material, by measuring polarization of the transmitted light [35], [36]; optical polarization, to measure stress in photoelastic materials [36] - [39]; and acoustics, to determine 3D temperature and velocity fields in furnaces [40], and velocity fields of heavy particles in plasma [41]. In other methodology, it has been shown that continuous Doppler data can also be analyzed in the framework of vector tomography [27], [42]-[46], [49].

As seen in the previous discussion, vector field tomography has been an active area of research for several applications including medical imaging. With all of this activity though, there has been little work in developing algorithms for the tomographic reconstruction of tensor fields, which has great potential for application in medical imaging. **Tensor field tomography** has been alluded to in the National Science Report [50] and in a review by Sparr and Strahlen [49]. We presented in [19] the results of computer simulations and results of an MRI diffusion experiment in which tensor tomography was applied in 2D. A general mathematical theory of integral geometry of tensor fields was presented in a monograph by Sharafutdinov [51] for general n-th order tensor fields with applications in integral geometry. A most interesting result presented in this monograph is that a symmetric tensor field also has a Helmholtz type decomposition in that it can be decomposed into a sum of a divergence-free component and a curl-free component. We show in this paper that for a 3D second order tensor field the solenoidal component can be expressed as the curl of a tensor potential and the irrotational component can be expressed as the gradient of a vector potential. This result is analogous to the Helmholtz decomposition of a vector field and to our knowledge has never been presented before in this form. Tomography also can be applied to more general frameworks - integral transforms of differential forms [52] and integral geometry of tensor fields - to find symmetric tensor fields from the integrals over all geodesics of a given Riemannian metric [51].

The **principles of scalar tomography** can fairly easily be extended to tensor

tomography. Though only second order tensors are considered in this paper the theory can be extended to nth-order tensors as well (see [53-56] for a general theory of tensor analysis). The scalar projection measurements of the tensor field are formed by creating inner products which are the products of a matrix multiplication of a unit directional vector before the tensor and after the tensor to give a scalar quantity at each point along the line of the projection measurement. Both analytical and iterative reconstruction algorithms can be used to reconstruct tensor fields, however we only consider an analytical approach in this paper. Analytical algorithms are appealing because they lend themselves better to a geometric interpretation of the physical problem. Iterative algorithms are appealing because they can perform better reconstructions when the data is limited or noisy.

In our initial work a reconstruction algorithm was developed for the reconstruction of two-dimensional tensor fields of second order tensors [19]. In this study, Fourier projection theorems were developed for the solenoidal and irrotational components of this 2x2 tensor. These algorithms were verified in computer simulations and applied to the reconstruction of two-dimensional diffusion tensor fields from MRI tensor projections. Here the 2D reconstruction algorithms are extended to 3D. Present work proposes a more general formulation of the decomposition for the case of 2D second order tensor fields.

This paper presents filter backprojection algorithms for reconstructing 3D second order tensor fields from either 3D planar or 3D line measurements. A Helmholtz-type of decomposition is proposed for tensor fields. Using this decomposition, a Fourier projection theorem is formulated in terms of the solenoidal and irrotational components of the tensor field. From that, it is shown that the solenoidal component of the tensor field can be reconstructed either from a single set of X-ray directional measurements, a single set of Radon directional measurements, or a combination of X-ray and Radon directional measurements. Results of computer simulations are presented. A diffusion tensor field in a cylindrical phantom intended to simulate the mid-ventricular region of the heart, was used in the simulations. The simulations verify the application's validity to the reconstruction three-dimensional tensor fields from Radon projections.

THEORY

Directional Projection Measurements of Tensor Fields

In reference to Figures 1 and 2, directional X-ray and Radon projections of tensor fields are defined. Let $\underline{x}=(x,y,z)$ be a point in $\Re^3$ and let the components $t_{ij}(\underline{x})$ of the tensor field $T(\underline{x})$ be real, rapidly decreasing C^∞ functions defined on $\Re^3$. For the tensor field

$$T(\underline{x})=\begin{bmatrix} t_{xx} & t_{xy} & t_{xz} \\ t_{yx} & t_{yy} & t_{yz} \\ t_{zx} & t_{zy} & t_{zz} \end{bmatrix}(\underline{x}) \quad , \tag{1}$$

the 3D directional X-ray transform of $T(\underline{x})$ is defined by

$$p^{\theta\tau}(\underline{s};\underline{\theta})=\int_{\Re}\sum_{i,j}\theta_i t_{ij}(\underline{s}+l\,\underline{\theta})\tau_j\,dl \quad , \tag{2a}$$

or

$$p^{\theta\tau}(\underline{s};\underline{\theta})=\int_{\Re}\underline{\theta}^T T(\underline{s}+l\,\underline{\theta})\underline{\tau}\,dl \quad , \tag{2b}$$

and the 3D directional Radon transformation of $T(\underline{x})$ is defined by

$$r^{\theta\tau}(t;\underline{\theta})=\int_{\Re^3}\sum_{i,j}\theta_i t_{ij}(\underline{x})\tau_j\,\delta(\underline{x}\cdot\underline{\theta}-t)\,d\underline{x} \quad , \tag{3a}$$

or

$$r^{\theta\tau}(t;\underline{\theta})=\int_{\Re^3}\underline{\theta}^T T(\underline{x})\underline{\tau}\,\delta(\underline{x}\cdot\underline{\theta}-t)\,d\underline{x} \quad , \tag{3b}$$

where $\underline{\theta},\underline{\tau}$ are three-dimensional directional unit vectors. These are directional projection measurements defined by the directional unit vectors $\underline{\theta},\underline{\tau}$. For vector fields, Prince [20] refers to

them as probe measurements. In 2D Braun and Hauck [32] identify projection measurements as transverse and longitudinal measurements, that correspond to the use of directional unit vectors $\underline{\theta}$ and $\underline{\theta}^{\perp}$, orthogonal to $\underline{\theta}$, respectively.

For the orthogonal vectors $\underline{\theta}$, $\underline{\alpha}$, and $\underline{\beta}$, we define the following directional Radon projection measurements as elements of the matrix

$$R(t;\underline{\theta}) = \begin{bmatrix} r^{\theta\theta} & r^{\theta\alpha} & r^{\theta\beta} \\ r^{\alpha\theta} & r^{\alpha\alpha} & r^{\alpha\beta} \\ r^{\beta\theta} & r^{\beta\alpha} & r^{\beta\beta} \end{bmatrix} (t;\theta) \quad , \tag{4}$$

and the directional X-ray projection measurements as elements of the matrix

$$P(u,v;\underline{\theta}) = \begin{bmatrix} p^{\theta\theta} & p^{\theta\alpha} & p^{\theta\beta} \\ p^{\alpha\theta} & p^{\alpha\alpha} & p^{\alpha\beta} \\ p^{\beta\theta} & p^{\beta\alpha} & p^{\beta\beta} \end{bmatrix} (u,v;\theta) \quad , \tag{5}$$

where

$$\underline{\theta} = (\sin\theta\cos\varphi, \sin\theta\sin\varphi, \cos\theta) \quad , \tag{6}$$

$$\underline{\alpha} = (-\sin\varphi, \cos\varphi, 0) \quad , \tag{7}$$

$$\underline{\beta} = (-\cos\theta\cos\varphi, -\cos\theta\sin\varphi, \sin\theta) \quad . \tag{8}$$

Projection Theorem for Directional X-ray Projections

The following derives a central section theorem (projection theorem) for the directional X-ray projection of a tensor field. For the derivation, we write the directional projection of a tensor field in the form of the integral of a matrix equation:

$$P(u,v;\underline{\theta}) = \int_{-\infty}^{\infty} \theta^T T(t\underline{\theta} + u\underline{\alpha} + v\underline{\beta})\theta \, dt \quad , \tag{9}$$

where $(t,u,v) \in \Re^3$, and

$$\theta = \begin{bmatrix} \sin\theta\cos\varphi & -\sin\varphi & -\cos\theta\cos\varphi \\ \sin\theta\sin\varphi & \cos\varphi & -\cos\theta\sin\varphi \\ \cos\theta & 0 & \sin\theta \end{bmatrix}, \tag{10}$$

and the columns of the matrix θ are the following three orthogonal directional vectors $\underline{\theta}$, $\underline{\alpha}$, and $\underline{\beta}$ defined in (6)-(8). Note that we use the notation without underline to denote the matrix θ and with the underline to denote the vector $\underline{\theta}$.

The Fourier transform of *P* is defined as

$$\tilde{P}(v_u, v_v; \underline{\theta}) = \int_{-\infty}^{\infty}\int_{-\infty}^{\infty} P(u, v; \underline{\theta}) e^{-2\pi i(uv_u + vv_v)} du dv, \tag{11}$$

where the Fourier transform of the matrix $P(u, v; \underline{\theta})$ is defined by taking the usual Fourier transform of each component. Substituting the expression for the directional projection of a tensor field, one obtains

$$\tilde{P}(v_u, v_v; \underline{\theta}) = \int_{-\infty}^{\infty}\int_{-\infty}^{\infty}\int_{-\infty}^{\infty} \theta^T T(t\theta + u\alpha + v\beta)\theta \, dt \, e^{-2\pi i(uv_u + vv_v)} du dv. \tag{12}$$

If we change variables $\underline{t} \rightarrow \underline{x}$, then

$$\tilde{P}(v_u, v_v; \underline{\theta}) = \int_{-\infty}^{\infty}\int_{-\infty}^{\infty}\int_{-\infty}^{\infty} \theta^T T(\underline{x})\theta \, e^{-2\pi i(\underline{x}\cdot\underline{\alpha} v_u + \underline{x}\cdot\underline{\beta} v_v)} d\underline{x}. \tag{13}$$

This leads to the following formulation of the central section theorem:

$$\tilde{P}(v_u, v_v; \underline{\theta}) = \theta^T \tilde{T}(\underline{\alpha} v_u + \underline{\beta} v_v)\theta, \tag{14}$$

or

$$\tilde{P}^{\theta\tau}(\underline{v}; \underline{\theta}) = \theta^T \tilde{T}(\underline{v})\theta, \tag{15}$$

where $\underline{v}\cdot\underline{\theta} = 0$ and $v = (v_t, v_u, v_v) \in \Re^3$.

Projection Theorem for Directional Radon Projections

In this section we derive a central section theorem (projection theorem) for the directional Radon projection of a tensor field. The following is the directional Radon projection of a tensor field in the form of the matrix equation

$$R(t;\underline{\theta})=\int_{-\infty}^{\infty}\theta^{T}T(t\underline{\theta}+u\underline{\alpha}+v\underline{\beta})\theta\,du\,dv \quad . \tag{16}$$

The Fourier transform of R is

$$\tilde{R}(v_t;\underline{\theta})=\int_{-\infty}^{\infty}R(t;\underline{\theta})e^{-2\pi i v_t t}\,dt \quad , \tag{17}$$

where t and v_t are elements of $\Re$. Substituting the expression for the directional projection of a tensor field, one obtains

$$\tilde{R}(v_t;\underline{\theta})=\int_{-\infty}^{\infty}\int_{-\infty}^{\infty}\int_{-\infty}^{\infty}\theta^{T}T(t\underline{\theta}+u\underline{\alpha}+v\underline{\beta})\theta\,du\,dv\,e^{-2\pi i v_t t}\,dt \quad . \tag{18}$$

If we change variables, $\underline{t} \rightarrow \underline{x}$, then

$$\tilde{R}(v_t;\underline{\theta})=\theta^{T}\left(\int_{-\infty}^{\infty}\int_{-\infty}^{\infty}\int_{-\infty}^{\infty}T(\underline{x})e^{-2\pi i v_t \underline{x}\cdot\underline{\theta}}\,d\underline{x}\right)\theta \quad . \tag{19}$$

This leads to the following formulation of the central section theorem for the directional Radon transform of a tensor field:

$$\tilde{R}(v_t;\underline{\theta})=\theta^{T}\tilde{T}(v_t\underline{\theta})\theta \quad . \tag{20}$$

Tensor Field Decomposition

It was shown by Sharafutdinov in [51], that a smooth symmetric tensor field which vanishes rapidly at infinity can be decomposed in a unique way as

$t_{ij}(\underline{x}) = t_{ij}^{S}(\underline{x}) + \frac{1}{2}\left(\partial_i \varphi_j(\underline{x}) + \partial_j \varphi_i(\underline{x})\right)$ where $\varphi(\underline{x})$ is a vector potential and $T_S(\underline{x})$ is a symmetric solenoidal tensor field, which is divergence free: $\sum_i \partial_i t_{ij}^{S}(\underline{x}) = \sum_j \partial_j t_{ij}^{S}(\underline{x}) = 0$. This is a generalization of the well-known vector field decomposition described by Helmholz [22]. Here we will consider a similar decomposition, but explicitly specify the solenoidal component as a curl of a tensor potential as is done in the Helmholz vector field decomposition.

We consider the following decomposition of a symmetric tensor field *T*:

$$T(\underline{x}) = T_{\Psi}^{S}(\underline{x}) + T_{\Phi}^{I}(\underline{x}) \quad , \tag{21}$$

where the solenoidal component $T_{\Psi}^{S}(\underline{x})$ is a symmetric tensor and is divergence free and $T_{\Phi}^{I}(\underline{x})$ is a symmetric tensor. The solenoidal and irrotational components will be specified as follows:

$$T_{\Psi}^{S}(\underline{x}) = \nabla \times \Psi(\underline{x}) \quad , \tag{22}$$

$$T_{\Phi}^{I}(\underline{x}) = \nabla \Phi(\underline{x}) + \left[\nabla \Phi(\underline{x})\right]^{T} \quad , \tag{23}$$

$$\Psi(\underline{x}) = \begin{bmatrix} 0 & \frac{\partial X_1}{\partial z} & -\frac{\partial X_1}{\partial y} \\ -\frac{\partial X_2}{\partial z} & 0 & \frac{\partial X_2}{\partial x} \\ \frac{\partial X_3}{\partial y} & -\frac{\partial X_3}{\partial x} & 0 \end{bmatrix}(\underline{x}) \quad , \tag{24}$$

where we define the notation $\nabla \times \Psi(\underline{x})$ as

$$\nabla\times\Psi(\underline{x})=\begin{bmatrix}\frac{\partial\Psi_{zx}}{\partial y}-\frac{\partial\Psi_{yx}}{\partial z} & \frac{\partial\Psi_{zy}}{\partial y}-\frac{\partial\Psi_{yy}}{\partial z} & \frac{\partial\Psi_{zz}}{\partial y}-\frac{\partial\Psi_{yz}}{\partial z}\\ \frac{\partial\Psi_{xx}}{\partial z}-\frac{\partial\Psi_{zx}}{\partial x} & \frac{\partial\Psi_{xy}}{\partial z}-\frac{\partial\Psi_{zy}}{\partial x} & \frac{\partial\Psi_{xz}}{\partial z}-\frac{\partial\Psi_{zz}}{\partial x}\\ \frac{\partial\Psi_{yx}}{\partial x}-\frac{\partial\Psi_{xx}}{\partial y} & \frac{\partial\Psi_{yy}}{\partial x}-\frac{\partial\Psi_{xy}}{\partial y} & \frac{\partial\Psi_{yz}}{\partial x}-\frac{\partial\Psi_{xz}}{\partial y}\end{bmatrix}(\underline{x}) \quad , \tag{25}$$

$$\Phi(\underline{x})=\begin{bmatrix}\Phi_1\\ \Phi_2\\ \Phi_3\end{bmatrix}(\underline{x}) \quad , \tag{26}$$

and

$$\nabla\Phi(\underline{x})=\begin{bmatrix}\frac{\partial}{\partial x}\\ \frac{\partial}{\partial y}\\ \frac{\partial}{\partial z}\end{bmatrix}\begin{bmatrix}\Phi_1 & \Phi_2 & \Phi_3\end{bmatrix}(\underline{x})=\begin{bmatrix}\frac{\partial\Phi_1}{\partial x} & \frac{\partial\Phi_2}{\partial x} & \frac{\partial\Phi_3}{\partial x}\\ \frac{\partial\Phi_1}{\partial y} & \frac{\partial\Phi_2}{\partial y} & \frac{\partial\Phi_3}{\partial y}\\ \frac{\partial\Phi_1}{\partial z} & \frac{\partial\Phi_2}{\partial z} & \frac{\partial\Phi_3}{\partial z}\end{bmatrix}(\underline{x}) \quad . \tag{27}$$

This combines the results of Sharafutdinov [51] with that of the Helmholtz decomposition for vector fields where the solenoidal is the curl of a vector potential and the irrotational component is the gradient of a scalar potential. From the above decomposition we see that for a second order tensor the solenoidal component is the curl of a tensor potential and the irrotational component is the gradient of a vector potential.

Now the Fourier transform of the tensor field decomposition gives

$$\widetilde{T}(\underline{\nu})=\widetilde{T}^{S}_{\Psi}(\underline{\nu})+\widetilde{T}^{I}_{\Phi}(\underline{\nu}) \quad , \tag{28}$$

where

$$\widetilde{T}^{S}_{\Psi}(\underline{\nu})=2\pi i[\underline{\nu}\times\widetilde{\Psi}(\underline{\nu})] \quad , \tag{29}$$

$$\tilde{T}^{I}_{\Phi}(\underline{v}) = 2\pi i[\underline{v}\tilde{\Phi}(\underline{v})] + 2\pi i[\underline{v}\tilde{\Phi}(\underline{v})]^{T} \quad , \tag{30}$$

and

$$\tilde{\Psi}(\underline{v}) = \begin{bmatrix} 0 & v_z \tilde{X}_1(\underline{v}) & -v_y \tilde{X}_1(\underline{v}) \\ -v_z \tilde{X}_2(\underline{v}) & 0 & v_x \tilde{X}_2(\underline{v}) \\ v_y \tilde{X}_3(\underline{v}) & -v_x \tilde{X}_3(\underline{v}) & 0 \end{bmatrix} \quad , \tag{31}$$

$$\tilde{\Phi}(\underline{v}) = \begin{bmatrix} \tilde{\Phi}_1 \\ \tilde{\Phi}_2 \\ \tilde{\Phi}_3 \end{bmatrix} (\underline{v}) \quad . \tag{32}$$

Note that the solenoidal component of the tensor field depends upon three scalar functions as does the irrotational component.

Since the divergence free condition for the solenoidal component of the tensor is $\sum_j v_j t^{S}_{ij}(v) = 0$, another way to interpret the decomposition is one of separating the components, in Fourier space, that are parallel to the frequency v. The solenoidal component is then given simply by projecting the Fourier transform of the tensor onto the plane orthogonal to v [51].

From the central section theorem for the directional **X-ray transform**, we know that

$$\tilde{P}(v_u, v_v; \underline{\theta}) = \begin{bmatrix} \tilde{p}^{\theta\theta} & \tilde{p}^{\theta\alpha} & \tilde{p}^{\theta\beta} \\ \tilde{p}^{\alpha\theta} & \tilde{p}^{\alpha\alpha} & \tilde{p}^{\alpha\beta} \\ \tilde{p}^{\beta\theta} & \tilde{p}^{\beta\alpha} & \tilde{p}^{\beta\beta} \end{bmatrix} (v_u, v_v; \underline{\theta}) = \theta^{T} \tilde{T}(v_u \underline{\alpha} + v_v \underline{\beta})\theta \quad . \tag{33}$$

Expanding the term on the right, we have

$$\tilde{P}(v_u, v_v; \underline{\theta}) = 2\pi i \theta^T \left[(v_u \underline{\alpha} + v_v \underline{\beta}) \times \tilde{\Psi}(v_u \underline{\alpha} + v_v \underline{\beta}) \right] \theta$$

$$+ 2\pi i \theta^T \left[(v_u \underline{\alpha} + v_v \underline{\beta}) \tilde{\Phi}(v_u \underline{\alpha} + v_v \underline{\beta}) \right] \theta$$

$$+ 2\pi i \theta^T \left[(v_u \underline{\alpha} + v_v \underline{\beta}) \tilde{\Phi}(v_u \underline{\alpha} + v_v \underline{\beta}) \right]^T \theta \qquad (34)$$

In the following we will evaluate the solenoidal and irrotational components of this expression.

For the **solenoidal** term, we have

$$\theta^T \tilde{T}^S_{\Psi}(v_u \underline{\alpha} + v_v \underline{\beta}) \theta = 2\pi i \theta^T \left[(v_u \underline{\alpha} + v_v \underline{\beta}) \times \tilde{\Psi}(v_u \underline{\alpha} + v_v \underline{\beta}) \right] \theta$$

$$= 2\pi i \begin{bmatrix} (\theta^T \tilde{T}^S_{\Psi} \theta)_{\theta\theta} & (\theta^T \tilde{T}^S_{\Psi} \theta)_{\theta\alpha} & (\theta^T \tilde{T}^S_{\Psi} \theta)_{\theta\beta} \\ (\theta^T \tilde{T}^S_{\Psi} \theta)_{\alpha\theta} & (\theta^T \tilde{T}^S_{\Psi} \theta)_{\alpha\alpha} & (\theta^T \tilde{T}^S_{\Psi} \theta)_{\alpha\beta} \\ (\theta^T \tilde{T}^S_{\Psi} \theta)_{\beta\theta} & (\theta^T \tilde{T}^S_{\Psi} \theta)_{\beta\alpha} & (\theta^T \tilde{T}^S_{\Psi} \theta)_{\beta\beta} \end{bmatrix} (v_u \underline{\alpha} + v_v \underline{\beta}) \quad , \qquad (35)$$

and for the **irrotational** term, we have

$$\theta^T \tilde{T}^I_{\Phi}(v_u \underline{\alpha} + v_v \underline{\beta}) \theta =$$

$$2\pi i \theta^T \left\{ (v_u \underline{\alpha} + v_v \underline{\beta}) \tilde{\Phi}(v_u \underline{\alpha} + v_v \underline{\beta}) + \left[(v_u \underline{\alpha} + v_v \underline{\beta}) \tilde{\Phi}(v_u \underline{\alpha} + v_v \underline{\beta}) \right]^T \right\} \theta$$

$$= 2\pi i \begin{bmatrix} (\theta^T \tilde{T}^I_{\Phi} \theta)_{\theta\theta} & (\theta^T \tilde{T}^I_{\Phi} \theta)_{\theta\alpha} & (\theta^T \tilde{T}^I_{\Phi} \theta)_{\theta\beta} \\ (\theta^T \tilde{T}^I_{\Phi} \theta)_{\alpha\theta} & (\theta^T \tilde{T}^I_{\Phi} \theta)_{\alpha\alpha} & (\theta^T \tilde{T}^I_{\Phi} \theta)_{\alpha\beta} \\ (\theta^T \tilde{T}^I_{\Phi} \theta)_{\beta\theta} & (\theta^T \tilde{T}^I_{\Phi} \theta)_{\beta\alpha} & (\theta^T \tilde{T}^I_{\Phi} \theta)_{\beta\beta} \end{bmatrix} (v_u \underline{\alpha} + v_v \underline{\beta}) \qquad (36)$$

Symbolically, we write the Fourier transform of the directional X-ray projection as

$$\tilde{P}(v_u, v_v; \underline{\theta}) = \begin{bmatrix} \tilde{p}^{\theta\theta} & \tilde{p}^{\theta\alpha} & \tilde{p}^{\theta\beta} \\ \tilde{p}^{\alpha\theta} & \tilde{p}^{\alpha\alpha} & \tilde{p}^{\alpha\beta} \\ \tilde{p}^{\beta\theta} & \tilde{p}^{\beta\alpha} & \tilde{p}^{\beta\beta} \end{bmatrix} (v_u, v_v; \underline{\theta}) = \begin{bmatrix} X & X & X \\ X & X & X \\ X & X & X \end{bmatrix} + \begin{bmatrix} 0 & X & X \\ X & X & X \\ X & X & X \end{bmatrix} \quad , \qquad (37)$$

where the solenoidal component (the first matrix) and the irrotational component (the second

matrix) are given in Appendix II.

From the central section theorem for the directional **Radon transform**, we know that

$$\widetilde{R}(v_t;\underline{\theta})=\begin{bmatrix}\widetilde{r}^{\theta\theta} & \widetilde{r}^{\theta\alpha} & \widetilde{r}^{\theta\beta}\\ \widetilde{r}^{\alpha\theta} & \widetilde{r}^{\alpha\alpha} & \widetilde{r}^{\alpha\beta}\\ \widetilde{r}^{\beta\theta} & \widetilde{r}^{\beta\alpha} & \widetilde{r}^{\beta\beta}\end{bmatrix}(v_t;\underline{\theta})=\theta^T\widetilde{T}(v_t\underline{\theta})\theta \quad .$$

(38)

Expressing this in terms of the decomposition, we have

$$\begin{aligned}\widetilde{R}(v_t;\underline{\theta})&=2\pi i\theta^T[(v_t\underline{\theta})\times\widetilde{\Psi}(v_t\underline{\theta})]\theta\\ &+2\pi i\theta^T[(v_t\underline{\theta})\widetilde{\Phi}(v_t\underline{\theta})]\theta\\ &+2\pi i\theta^T[(v_t\underline{\theta})\widetilde{\Phi}(v_t\underline{\theta})]^T\theta\end{aligned} \tag{39}$$

Again in the following we evaluate the solenoidal and irrotational components of this expression.

For the **solenoidal** component, we have

$$\begin{aligned}\widetilde{T}^S_{\Psi}(v_t\underline{\theta})&=2\pi i\theta^T[(v_t\underline{\theta})\times\widetilde{\Psi}(v_t\underline{\theta})]\theta\\ &=2\pi i\begin{bmatrix}(\theta^T\widetilde{T}^S_{\Psi}\theta)_{\theta\theta} & (\theta^T\widetilde{T}^S_{\Psi}\theta)_{\theta\alpha} & (\theta^T\widetilde{T}^S_{\Psi}\theta)_{\theta\beta}\\ (\theta^T\widetilde{T}^S_{\Psi}\theta)_{\alpha\theta} & (\theta^T\widetilde{T}^S_{\Psi}\theta)_{\alpha\alpha} & (\theta^T\widetilde{T}^S_{\Psi}\theta)_{\alpha\beta}\\ (\theta^T\widetilde{T}^S_{\Psi}\theta)_{\beta\theta} & (\theta^T\widetilde{T}^S_{\Psi}\theta)_{\beta\alpha} & (\theta^T\widetilde{T}^S_{\Psi}\theta)_{\beta\beta}\end{bmatrix}(v_t\underline{\theta})\end{aligned}$$

(40)

and for the **irrotational** component, we have

$$\begin{aligned}\widetilde{T}^I_{\Phi}(v_t\underline{\theta})&=2\pi i\theta^T\{(v_t\underline{\theta})\widetilde{\Phi}(v_t\underline{\theta})+[(v_t\underline{\theta})\widetilde{\Phi}(v_t\underline{\theta})]^T\}\theta\\ &=2\pi i\begin{bmatrix}(\theta^T\widetilde{T}^I_{\Phi}\theta)_{\theta\theta} & (\theta^T\widetilde{T}^I_{\Phi}\theta)_{\theta\alpha} & (\theta^T\widetilde{T}^I_{\Phi}\theta)_{\theta\beta}\\ (\theta^T\widetilde{T}^I_{\Phi}\theta)_{\alpha\theta} & (\theta^T\widetilde{T}^I_{\Phi}\theta)_{\alpha\alpha} & (\theta^T\widetilde{T}^I_{\Phi}\theta)_{\alpha\beta}\\ (\theta^T\widetilde{T}^I_{\Phi}\theta)_{\beta\theta} & (\theta^T\widetilde{T}^I_{\Phi}\theta)_{\beta\alpha} & (\theta^T\widetilde{T}^I_{\Phi}\theta)_{\beta\beta}\end{bmatrix}(v_t\underline{\theta})\end{aligned}$$

(41)

Symbolically, we write the Fourier transform of the directional Radon projection as

$$\widetilde{R}(v_t;\underline{\theta})=\begin{bmatrix}\widetilde{r}^{\theta\theta} & \widetilde{r}^{\theta\alpha} & \widetilde{r}^{\theta\beta}\\ \widetilde{r}^{\alpha\theta} & \widetilde{r}^{\alpha\alpha} & \widetilde{r}^{\alpha\beta}\\ \widetilde{r}^{\beta\theta} & \widetilde{r}^{\beta\alpha} & \widetilde{r}^{\beta\beta}\end{bmatrix}(v_t;\underline{\theta})=\begin{bmatrix}0 & 0 & 0\\ 0 & X & X\\ 0 & X & X\end{bmatrix}+\begin{bmatrix}X & X & X\\ X & 0 & 0\\ X & 0 & 0\end{bmatrix},$$

(42)

where the solenoidal component (the first matrix) and the irrotational component (the second matrix) are given in Appendix III.

From (37) and (43), one can make the following statements: Statement 1. Measurement of $p^{\theta\theta}$ on one Orlov circle [85] and measurement of $r^{\alpha\alpha}$ and $r^{\beta\beta}$ over 4π will specify the solenoidal component. Statement 2. Measurement of $p^{\theta\theta}$ on three Orlov's circles will specify the solenoidal component. Statement 3. Measurement of $r^{\theta\theta}$, $r^{\theta\alpha}$, and $r^{\theta\beta}$ over 4π will specify the irrotational component. Statement 4. Measurement of $r^{\alpha\alpha}$, $r^{\alpha\beta}$, and $r^{\beta\beta}$ over 4π will specify the solenoidal component.

<u>Tensor Field Reconstruction Using Directional Radon Projections</u>

In developing reconstruction formulae for tensor fields, we will first consider the straightforward reconstruction of the elements of the tensor field from directional Radon projection measurements. The following sections will give formulae for the reconstruction of solenoidal and irrotational components of the tensor field. From (16), we can write

$$R(t;\underline{\theta})=\theta^T\begin{bmatrix}\hat{t}_{xx} & \hat{t}_{xy} & \hat{t}_{xz}\\ \hat{t}_{yx} & \hat{t}_{yy} & \hat{t}_{yz}\\ \hat{t}_{zx} & \hat{t}_{zy} & \hat{t}_{zz}\end{bmatrix}(t;\underline{\theta})\theta \quad ¿\theta^T\hat{T}(t;\underline{\theta})\theta,$$

(43)

where $\hat{t}_{ij}(t;\underline{\theta})$ are the projections of each individual tensor component. Solving the matrix

equation for $\hat{T}$, we have

$$\hat{T}(t;\theta)=\begin{bmatrix}\hat{t}_{xx} & \hat{t}_{xy} & \hat{t}_{xz}\\ \hat{t}_{yx} & \hat{t}_{yy} & \hat{t}_{yz}\\ \hat{t}_{zx} & \hat{t}_{zy} & \hat{t}_{zz}\end{bmatrix}(t;\underline{\theta})=\theta R(t;\underline{\theta})\theta^T \quad .$$

(44)

The reconstuction can be written using Radon's inversion formula:

$$T(\underline{x})=-\frac{1}{8\pi^2}\iint_{4\pi}\frac{\partial^2}{\partial t^2}\theta R(\underline{x}\cdot\underline{\theta};\underline{\theta})\theta^T\sin(\theta)d\theta d\varphi \quad . \qquad (45)$$

The expression in (45) gives an equation for the reconstruction of each element of the tensor in terms of the Radon inverse of a linear sum of directional Radon projection measurements.

Solenoidal Reconstruction Using Directional Radon Projections $r^{\alpha\alpha}$, $r^{\alpha\beta}$, and $r^{\beta\beta}$

Next we consider the reconstruction of solenoidal and irrotational components of the tensor field. We derive an algorithm for the reconstruction of the solenoidal component of the tensor field from directional Radon projections, which are the solenoidal Radon measurements. From the projection theorem we have the following three equations (C7), (C8), and (C11) that give the Fourier transform of the directional Radon projections $r^{\alpha\alpha}$, $r^{\alpha\beta}$, and $r^{\beta\beta}$ in terms of the Fourier transform of the three unknowns X_1 , X_2 , and X_3 of the tensor potential. Writing this in matrix notation gives the following matrix equation (**change the sign in the second column**):

$$\begin{bmatrix}\widetilde{r}^{\alpha\alpha}\\ \widetilde{r}^{\alpha\beta}\\ \widetilde{r}^{\beta\beta}\end{bmatrix}(v_t;\underline{\theta})=2\pi i v_t^2\begin{bmatrix}\cos^2\theta\cos^2\varphi & -\cos^2\theta\sin^2\varphi & \sin^2\theta\\ -\frac{1}{2}\cos(\theta)\sin(2\varphi) & -\frac{1}{2}\cos(\theta)\sin(2\varphi) & 0\\ \sin^2\varphi & -\cos^2\varphi & 0\end{bmatrix}\begin{bmatrix}\widetilde{X}_1\\ \widetilde{X}_2\\ \widetilde{X}_3\end{bmatrix}(v_t\underline{\theta}) \qquad .(46)$$

Solving for $\widetilde{X}_1$, $\widetilde{X}_2$, and $\widetilde{X}_3$, we have

$$\begin{bmatrix} \widetilde{X}_1 \\ \widetilde{X}_2 \\ \widetilde{X}_3 \end{bmatrix}(v_t \underline{\theta}) = \frac{1}{2\pi i v_t^2} \begin{bmatrix} 0 & -\sec(\theta)\cot(\varphi) & 1 \\ 0 & -\sec(\theta)\tan(\varphi) & -1 \\ \csc^2(\theta) & 2\cot(\theta)\csc(\theta)\cot(2\varphi) & -\cot^2(\theta) \end{bmatrix} \begin{bmatrix} \widetilde{r}^{\alpha\alpha} \\ \widetilde{r}^{\alpha\beta} \\ \widetilde{r}^{\beta\beta} \end{bmatrix}(v_t; \underline{\theta}) \quad .$$

(47)

If $C_i^{\xi\zeta}$ are the elements of the matrix in (47), then we have the following expression for the second derivative of the projections $\hat{X}_i$ of the elements of the tensor potential

$$\frac{\partial^2 \hat{X}_i}{\partial t^2}(t; \underline{\theta}) = C_i^{\alpha\alpha} r^{\alpha\alpha}(t; \underline{\theta}) + C_i^{\alpha\beta} r^{\alpha\beta}(t; \underline{\theta}) + C_i^{\beta\beta} r^{\beta\beta}(t; \underline{\theta}) \quad . \qquad (48)$$

From the Radon inversion formula

$$X_i(\underline{x}) = -\frac{1}{8\pi^2} \iint_{4\pi} \frac{\partial^2}{\partial t^2} \hat{X}(\underline{x} \cdot \underline{\theta}; \underline{\theta}) \sin(\theta) d\theta d\varphi \quad ,$$

(49)

we have the following expression for the reconstruction of the elements of the tensor potential

$$X_i(\underline{x}) = -\frac{1}{8\pi^2} \iint_{4\pi} [\, C_i^{\alpha\alpha} r^{\alpha\alpha}(\underline{x} \cdot \underline{\theta}; \underline{\theta}) + C_i^{\alpha\beta} r^{\alpha\beta}(\underline{x} \cdot \underline{\theta}; \underline{\theta}) + C_i^{\beta\beta} r^{\beta\beta}(\underline{x} \cdot \underline{\theta}; \underline{\theta}) \,] \sin(\theta) d\theta d\varphi \quad .$$

(50)

The expression in (50) gives a weighted backprojection-type algorithm for reconstructing the tensor potential components X_1 , X_2 , and X_3 . The algorithm involves the backprojection of a weighted sum of the solenoidal Radon measurements. Note to reconstruct the tensor potential elements X_1 , X_2 , and X_3 no filtering is required as is the case in scalar tomography.

Irrotational Reconstruction Using Directional Radon Projections $r^{\theta\theta}$, $r^{\theta\alpha}$, and $r^{\theta\beta}$

Next we look at the reconstruction of the irrotational component of the tensor field from directional Radon projections. From the projection theorem we have the following three equations (C13), (C14), and (C15) that give the Fourier transform of the directional Radon projections $r^{\theta\theta}$

, $r^{\theta\alpha}$, and $r^{\theta\beta}$ (the irrotational Radon measurements) in terms of the Fourier transform of the three unknowns Φ_1 , Φ_2 , and Φ_3 of the vector potential. Writing this in matrix notation gives the following matrix equation:

$$\begin{bmatrix} \tilde{r}^{\theta\theta} \\ \tilde{r}^{\theta\alpha} \\ \tilde{r}^{\theta\beta} \end{bmatrix}(v_t;\underline{\theta}) = 2\pi i v_t \begin{bmatrix} 2\sin(\theta)\cos(\varphi) & 2\sin(\theta)\sin(\varphi) & 2\cos(\theta) \\ -\sin(\varphi) & \cos(\varphi) & 0 \\ -\cos(\theta)\cos(\varphi) & -\cos(\theta)\sin(\varphi) & \sin(\theta) \end{bmatrix} \begin{bmatrix} \tilde{\Phi}_1 \\ \tilde{\Phi}_2 \\ \tilde{\Phi}_3 \end{bmatrix}(v_t\underline{\theta}) \quad . \qquad (51)$$

Solving for $\tilde{\Phi}_1$, $\tilde{\Phi}_2$, and $\tilde{\Phi}_3$ we have

$$\begin{bmatrix} \tilde{\Phi}_1 \\ \tilde{\Phi}_2 \\ \tilde{\Phi}_3 \end{bmatrix}(v_t\underline{\theta}) = \frac{1}{2\pi i v_t} \begin{bmatrix} \frac{\sin(\theta)\cos(\varphi)}{2} & -\sin(\varphi) & -\cos(\theta)\cos(\varphi) \\ \frac{\sin(\theta)\sin(\varphi)}{2} & \cos(\varphi) & -\cos(\theta)\sin(\varphi) \\ \frac{\cos(\theta)}{2} & 0 & \sin(\theta) \end{bmatrix} \begin{bmatrix} \tilde{r}^{\theta\theta} \\ \tilde{r}^{\theta\alpha} \\ \tilde{r}^{\theta\beta} \end{bmatrix}(v_t;\underline{\theta}) \quad . \qquad (52)$$

If $C_i^{\xi\zeta}$ are the elements of the matrix in (49), then we have the following expression for the derivative of the projections $\hat{\Phi}_i$ of the elements of the vector potential

$$\frac{\partial \hat{\Phi}_i}{\partial t}(t;\underline{\theta}) = C_i^{\theta\theta} r^{\theta\theta}(t;\underline{\theta}) + C_i^{\theta\alpha} r^{\theta\alpha}(t;\underline{\theta}) + C_i^{\theta\beta} r^{\theta\beta}(t;\underline{\theta}) \quad . \qquad (53)$$

From the Radon inversion formula

$$\Phi_i(\underline{x}) = -\frac{1}{8\pi^2}\iint_{4\pi} \frac{\partial^2}{\partial t^2}\hat{\Phi}(\underline{x}\cdot\underline{\theta};\underline{\theta})\sin(\theta)\,d\theta d\varphi \quad , \qquad (54)$$

we have the following expression for the reconstruction of the elements of the vector potential

$$\Phi_i(\underline{x}) = -\frac{1}{8\pi^2}\iint_{4\pi} \frac{\partial}{\partial t}\left[C_i^{\theta\theta}\frac{r^{\theta\theta}(\underline{x}\cdot\underline{\theta};\underline{\theta})}{2} + C_i^{\theta\alpha} r^{\theta\alpha}(\underline{x}\cdot\underline{\theta};\underline{\theta}) + C_i^{\theta\beta} r^{\theta\beta}(\underline{x}\cdot\underline{\theta};\underline{\theta})\right]\sin(\theta)\,d\theta d\varphi \quad . \qquad (55)$$

The expression in (55) is a filtered backprojection-type algorithm. The filter is a first derivative operation that differs from the normal second derivative filter obtained from the Radon inversion. We see that the reconstruction of the components Φ_1 , Φ_2 , and Φ_3 of the vector potential of the irrotational component is given in terms of the backprojection of the derivative of the weighted sum of the irrotational Radon measurements.

Solenoidal Reconstruction Using Directional X-Ray Projections $p^{\theta\theta}$, and Directional Radon Projections $r^{\alpha\alpha}$, and $r^{\beta\beta}$

We see from the expressions above that the solenoidal component can be reconstructed from totally solenoidal Radon measurements or from totally solenoidal X-ray measurements. The natural question is can these be combined in a way to give another reconstruction formula for the reconstruction of the solenoidal component in terms of a combination of directional Radon and directional X-ray measurements? In this section we derive a filtered backprojection algorithm for the reconstruction of the solenoidal component of the tensor field from a combination of such measurements. From the projection theorem we have the following three equations (B3), (C7), and (C11) that give the Fourier transform of the directional X-ray projection $\tilde{p}^{\theta\theta}$ and the directional Radon projections $\tilde{r}^{\alpha\alpha}$ and $\tilde{r}^{\beta\beta}$ in terms of the Fourier transform of the three unknowns X_1 , X_2 , and X_3 of the tensor potential:

$$\tilde{p}^{\theta\theta}(v_u\underline{\alpha}+v_v\underline{\beta};\underline{\theta})= 2\pi i[(\cos(\theta)\cos(\varphi)v_u-\sin(\varphi)v_v)^2\tilde{X}_1-(\cos(\theta)\sin(\varphi)v_u+\cos(\varphi)v_v)^2\tilde{X}_2+\sin^2(\theta)v_u^2\tilde{X}_3](v_u\underline{\alpha}+v_v\underline{\beta}) \quad (56)$$

$$\tilde{r}^{\alpha\alpha}(v_t;\underline{\theta}')=2\pi i v_t^2[\cos^2(\theta')\cos^2(\varphi')\tilde{X}_1(v_t\underline{\theta}')-\cos^2(\theta')\sin^2(\varphi')\tilde{X}_2(v_t\underline{\theta}')+\sin^2(\theta')\tilde{X}_3(v_t\underline{\theta}')] , \quad (57)$$

$$\tilde{r}^{\beta\beta}(v_t;\underline{\theta}') = 2\pi i v_t^2[\sin^2(\varphi')\tilde{X}_1(v_t\underline{\theta}') - \cos^2(\varphi')\tilde{X}_2(v_t\underline{\theta}')] \quad , \tag{58}$$

where $v_t\underline{\theta}' = v_u\underline{\alpha} + v_v\underline{\beta}$. Writing this in matrix notation gives the following matrix equation:

$$\begin{bmatrix} \tilde{p}^{\theta\theta}(v_u, v_v;\underline{\theta}) \\ \tilde{r}^{\alpha\alpha}(v_t;\underline{\theta}') \\ \tilde{r}^{\beta\beta}(v_t;\underline{\theta}') \end{bmatrix} = 2\pi i \begin{bmatrix} (\cos(\theta)\cos(\varphi)v_u - \sin(\varphi)v_v)^2 & -(\cos(\theta)\sin(\varphi)v_u + \cos(\varphi)v_v)^2 & \sin^2(\theta)v_u^2 \\ \frac{v_{v^2}\sin^2(\theta)(v_u\sin\varphi + v_v\cos\theta\cos\varphi)^2}{v_{u^2} + v_{v^2}\cos^2\theta} & \frac{-v_{v^2}\sin^2(\theta)(v_u\cos\varphi - v_v\cos\theta\sin\varphi)^2}{v_{u^2} + v_{v^2}\cos^2\theta} & v_{u^2} + v_{v^2}\cos^2\theta \\ \frac{(v_{u^2} + v_{v^2})(v_u\cos\varphi - v_v\cos\theta\sin\varphi)^2}{v_{u^2} + v_{v^2}\cos^2\theta} & \frac{-(v_{u^2} + v_{v^2})(v_u\sin\varphi + v_v\cos\theta\cos\varphi)^2}{v_{u^2} + v_{v^2}\cos^2\theta} & 0 \end{bmatrix} \begin{bmatrix} \tilde{X}_1 \\ \tilde{X}_2 \\ \tilde{X}_3 \end{bmatrix}(v_t\underline{\theta}') \tag{59}$$

Solving for $\tilde{X}_1$, $\tilde{X}_2$, and $\tilde{X}_3$, we have

$$\begin{bmatrix} \tilde{X}_1 \\ \tilde{X}_2 \\ \tilde{X}_3 \end{bmatrix}(v_t\underline{\theta}') = \frac{1}{2\pi i}\begin{bmatrix} \tilde{C}_1^{\theta\theta} & \tilde{C}_1^{\alpha\alpha} & \tilde{C}_1^{\beta\beta} \\ \tilde{C}_2^{\theta\theta} & \tilde{C}_2^{\alpha\alpha} & \tilde{C}_2^{\beta\beta} \\ \tilde{C}_3^{\theta\theta} & \tilde{C}_3^{\alpha\alpha} & \tilde{C}_3^{\beta\beta} \end{bmatrix}\begin{bmatrix} \tilde{p}^{\theta\theta}(v_u, v_v;\underline{\theta}) \\ \tilde{r}^{\alpha\alpha}(v_t;\underline{\theta}') \\ \tilde{r}^{\beta\beta}(v_t;\underline{\theta}') \end{bmatrix} \quad , \tag{60}$$

where $\tilde{C}_i^{\xi\zeta}$ are elements of the Fourier transform of the matrix C . The matrix $\tilde{C}$ is presented in the following Mathematica format:

$$\left\{\left\{-\frac{\mathrm{Sec}[\theta]\,(\mathrm{Csc}[\theta]\,\mathrm{Sin}[\phi]\,\nu_u+\mathrm{Cos}[\phi]\,\mathrm{Cot}[\theta]\,\nu_v)^2\,(\nu_u^2+\mathrm{Cos}[\theta]^2\,\nu_v^2)}{\nu_u\,\nu_v\,(\nu_u^2+\nu_v^2)\,(\mathrm{Sin}[2\phi]\,\nu_u^2+2\,\mathrm{Cos}[\theta]\,\mathrm{Cos}[2\phi]\,\nu_u\,\nu_v-\mathrm{Cos}[\theta]^2\,\mathrm{Sin}[2\phi]\,\nu_v^2)},\right.\right.$$
$$\frac{\mathrm{Sec}[\theta]\,\nu_u\,(\mathrm{Sin}[\phi]\,\nu_u+\mathrm{Cos}[\theta]\,\mathrm{Cos}[\phi]\,\nu_v)^2}{\nu_v\,(\nu_u^2+\nu_v^2)\,(\mathrm{Sin}[2\phi]\,\nu_u^2+2\,\mathrm{Cos}[\theta]\,\mathrm{Cos}[2\phi]\,\nu_u\,\nu_v-\mathrm{Cos}[\theta]^2\,\mathrm{Sin}[2\phi]\,\nu_v^2)},$$
$$\left.\left.\frac{\mathrm{Csc}[\theta]^2\,(2\,\mathrm{Cos}[\theta]\,\mathrm{Sin}[\phi]\,\nu_u^3-(-3+\mathrm{Cos}[2\theta])\,\mathrm{Cos}[\phi]\,\nu_u^2\,\nu_v+(\mathrm{Cos}[\theta]+\mathrm{Cos}[3\theta])\,\mathrm{Sin}[\phi]\,\nu_u\,\nu_v^2+2\,\mathrm{Cos}[\theta]^2\,\mathrm{Cos}[\phi]\,\nu_v^3)}{4\,\nu_u\,\nu_v\,(\mathrm{Cos}[\phi]\,\nu_u-\mathrm{Cos}[\theta]\,\mathrm{Sin}[\phi]\,\nu_v)\,(\nu_u^2+\nu_v^2)}\right\},$$
$$\left\{-\frac{\mathrm{Sec}[\theta]\,(\mathrm{Cos}[\phi]\,\mathrm{Csc}[\theta]\,\nu_u-\mathrm{Cot}[\theta]\,\mathrm{Sin}[\phi]\,\nu_v)^2\,(\nu_u^2+\mathrm{Cos}[\theta]^2\,\nu_v^2)}{\nu_u\,\nu_v\,(\nu_u^2+\nu_v^2)\,(\mathrm{Sin}[2\phi]\,\nu_u^2+2\,\mathrm{Cos}[\theta]\,\mathrm{Cos}[2\phi]\,\nu_u\,\nu_v-\mathrm{Cos}[\theta]^2\,\mathrm{Sin}[2\phi]\,\nu_v^2)},\right.$$
$$\frac{\mathrm{Sec}[\theta]\,\nu_u\,(\mathrm{Cos}[\phi]\,\nu_u-\mathrm{Cos}[\theta]\,\mathrm{Sin}[\phi]\,\nu_v)^2}{\nu_v\,(\nu_u^2+\nu_v^2)\,(\mathrm{Sin}[2\phi]\,\nu_u^2+2\,\mathrm{Cos}[\theta]\,\mathrm{Cos}[2\phi]\,\nu_u\,\nu_v-\mathrm{Cos}[\theta]^2\,\mathrm{Sin}[2\phi]\,\nu_v^2)},$$
$$\left.\frac{\mathrm{Csc}[\theta]^2\,(2\,\mathrm{Cos}[\theta]\,\mathrm{Cos}[\phi]\,\nu_u^3+(-3+\mathrm{Cos}[2\theta])\,\mathrm{Sin}[\phi]\,\nu_u^2\,\nu_v+(\mathrm{Cos}[\theta]+\mathrm{Cos}[3\theta])\,\mathrm{Cos}[\phi]\,\nu_u\,\nu_v^2-2\,\mathrm{Cos}[\theta]^2\,\mathrm{Sin}[\phi]\,\nu_v^3)}{4\,\nu_u\,\nu_v\,(\mathrm{Sin}[\phi]\,\nu_u+\mathrm{Cos}[\theta]\,\mathrm{Cos}[\phi]\,\nu_v)\,(\nu_u^2+\nu_v^2)}\right\},$$
$$\left\{\frac{\nu_v\,(-\mathrm{Cos}[2\phi]\,\mathrm{Sec}[\theta]\,\nu_u^2+2\,\mathrm{Sin}[2\phi]\,\nu_u\,\nu_v+\mathrm{Cos}[\theta]\,\mathrm{Cos}[2\phi]\,\nu_v^2)}{\nu_u\,(\nu_u^2+\nu_v^2)\,(\mathrm{Sin}[2\phi]\,\nu_u^2+2\,\mathrm{Cos}[\theta]\,\mathrm{Cos}[2\phi]\,\nu_u\,\nu_v-\mathrm{Cos}[\theta]^2\,\mathrm{Sin}[2\phi]\,\nu_v^2)},\right.$$
$$\frac{2\,\mathrm{Sin}[2\phi]\,\nu_u^2+(3+\mathrm{Cos}[2\theta])\,\mathrm{Cos}[2\phi]\,\mathrm{Sec}[\theta]\,\nu_u\,\nu_v-2\,\mathrm{Sin}[2\phi]\,\nu_v^2}{2\,(\nu_u^2+\nu_v^2)\,(\mathrm{Sin}[2\phi]\,\nu_u^2+2\,\mathrm{Cos}[\theta]\,\mathrm{Cos}[2\phi]\,\nu_u\,\nu_v-\mathrm{Cos}[\theta]^2\,\mathrm{Sin}[2\phi]\,\nu_v^2)},$$
$$\left.\left.\frac{1}{-2\,\nu_u^2-2\,\mathrm{Cos}[\theta]\,\mathrm{Cot}[\phi]\,\nu_u\,\nu_v}+\frac{1}{\nu_u^2+\nu_v^2}+\frac{1}{-2\,\nu_u^2+2\,\mathrm{Cos}[\theta]\,\nu_u\,\nu_v\,\mathrm{Tan}[\phi]}\right\}\right\}$$

If $\hat{\tilde{X}}_i^{\theta\theta}(\nu_u,\nu_v;\underline{\theta})=\tilde{C}_i^{\theta\theta}(\nu_u,\nu_v)\,\tilde{p}^{\theta\theta}(\nu_u,\nu_v;\underline{\theta})$, $\tilde{X}_i^{\alpha\alpha}(\nu_t;\theta')=\tilde{C}_i^{\alpha\alpha}(\nu_t)\,\tilde{r}^{\alpha\alpha}(\nu_t;\underline{\theta}')$, and $\tilde{X}_i^{\beta\beta}(\nu_t;\theta')=\tilde{C}_i^{\beta\beta}(\nu_t)\,\tilde{r}^{\beta\beta}(\nu_t;\underline{\theta}')$ then we have the Fourier inverse of these components giving the filtered directional projections: $X_i^{\theta\theta}(u,v;\underline{\theta})=C_i^{\theta\theta}\otimes p^{\theta\theta}(u,v;\underline{\theta})$, $X_i^{\alpha\alpha}(t;\underline{\theta}')=C_i^{\alpha\alpha}(t)\otimes r^{\alpha\alpha}(t;\underline{\theta}')$, and $X_i^{\beta\beta}(t;\underline{\theta}')=C_i^{\beta\beta}(t)\otimes r^{\beta\beta}(t;\underline{\theta}')$. Note the difference in arguments between the filtered directional Radon projections and the filtered directional X-ray projections. Since these are filtered projections the backprojection gives us the following reconstruction of the elements of the tensor potential:

$$X_i(\underline{x})=\iint_{\Omega}[X_i^{\theta\theta}(\underline{x}\cdot\underline{\alpha},\underline{x}\cdot\underline{\beta};\underline{\theta})]\sin(\theta)\,d\theta d\varphi$$
$$+\iint_{\Omega}[X_i^{\alpha\alpha}(\underline{x}\cdot\underline{\theta}';\underline{\theta}')+\hat{X}_i^{\beta\beta}(\underline{x}\cdot\underline{\theta}';\underline{\theta}')]\sin(\theta')\,d\theta'd\varphi \quad . \qquad (61)$$

Note that the coefficients $C_i^{\xi\zeta}$ are Fourier inverses of $\tilde{C}_i^{\xi\zeta}$ which are fairly complex expressions. In implementing such an algorithm it may be easier to perform the filtering first in frequency space then perform the Fourier inverse followed by the backprojection given in (61).

DISCUSSION

Reconstruction formulae are presented for reconstructing solenoidal and irrotational components of 3D tensor fields from directional Radon and X-ray projections. Fourier projection theorems were derived for the irrotational and solenoidal components of the tensor field. The Fourier projection theorems provide relationships between the solenoidal and irrotational components and the directional projection measurements for X-ray and Radon measurements. These relationships illustrate which directional measurements are totally related to the solenoidal component and which are totally related to the irrotational component. These relationships show how the projections of a tensor field are to be sampled in order to recover the full tensor field and they lead to easy derivations of Fourier, filtered backprojection, and convolution backprojection reconstruction algorithms. This work provides a framework and structure to tensor tomography experiments that can be useful for application of either analytical filter backprojection or iterative reconstruction algorithms in the processing of acquired data. If appropriate projections cannot be formed from an experiment (for example, approximations which are required for MRI diffusion projection data) then those projections can be processed by iterative algorithms. Iterative reconstruction algorithms are also appropriate for reconstruction of 3D tensor fields using the same techniques previously implemented for reconstruction of 2D vector fields [21,40,47,48].

Even though formulations are given for the reconstruction of 3D second order tensor fields from both directional Radon and directional X-ray measurements, only results of simulations using **directional Radon projections** are provided. The implementation of 3D reconstructions from directional X-ray projections can be more complicated since the filtering depends upon very general projection sampling schemes that must include a great circle. This is an area of research that will be investigated in the future. Also, the formulations for the reconstruction of tensor fields from a mixture of directional Radon and directional X-ray projections suggest the potential for future algorithm investigations.

The reconstruction of tensor fields is **computationally** more involved than the reconstruction of scalar fields. Even though the tensor was symmetric in our simulations, we reconstructed all nine components of the tensor field. The reconstructions of the $32 \times 32 \times 32$

tensor fields required approximately one hour. This included time to simulate the projections. The reconstruction of the nine elements took more than nine times the time to perform one scalar reconstruction because of the additional multiplications of sines and cosines in the expression given in (45).

The approach taken in this study was to **decompose** the tensor field into a curl of a tensor potential (solenoidal component) and a gradient of a vector potential (irrotational component). This decomposition directly relates to tomography. The decomposition is not necessary for obtaining a reconstruction algorithm for tensor fields however it provides a window into what tomography may be used for and what it may help to accomplish. The decomposition shows what projection samples affect each component of the decomposition. In the case of 2D vector tomography, Braun and Hauck [32] showed that the longitudinal and transverse measurements, which correspond to the use of directional measurements equal to $\underline{\theta}$ and orthogonal to $\underline{\theta}^{\perp}$, reconstruct the irrotational and solenoidal components of a vector field, respectively. In three dimensions, one might consider longitudinal measurements to be along θ and transverse measurements are clear once the two transverse vectors are specified for which the choice is not unique. Prince [20] used the expression irrotational measurements to refer to the probe transform acquired using the probe $p=\underline{\theta}$ (directional Radon transform r^{θ} of a vector field in our terminology). Similarly, he used the expression solenoidal measurements to refer to the pair of probe transform measurements acquired using probes $p_1=\underline{\alpha}$ and $p_2=\underline{\beta}$, which are both orthogonal to $\underline{\theta}$. Here we see that for tensor fields the directional Radon transforms, $r^{\theta\theta}$, $r^{\theta\alpha}$, and $r^{\theta\beta}$, are solenoidal measurements and $r^{\alpha\alpha}$, $r^{\alpha\beta}$, and $r^{\beta\beta}$ are the irrotational measurements.

Sharafutdinov does explicitly represent the solenoid part in terms of X_1, X_2, X_3 as in equation (13). Even thought this representation is elegant, it brings a number of problems that are apparent in the paper. First there is no proof that this decomposition always exists with well-

behaved functions $X_1(x,y,z),\quad X_2(x,y,z),\quad X_3(x,y,z)$. Second the X_i 's have no intuitive physical meaning. Third the vector (X_1, X_2, X_3) is not a vector that is it does not transform as a vector when you rotate the system of coordinates, which further undermine any intuitive meaning. Fourth and more importantly, the calculation of the X_i 's involves singularities, which are apparent from $\sec(\theta)$ and $\cot(\varphi)$ in equation (50). Hence the integral over θ and φ in equation (53) is not defined (I do not think that these singularities are integrable) unless maybe if the data are noise-free (consistent). This means that equation (53) is not well defined. However, the decomposition in X_i 's is not used in the simulations which directly reconstructs the solenoid part of the tensor.

The decomposition can be especially useful in an MRI experiment. If the diffusion tensor field is totally solenoidal (as is almost the case for the simulation we used in this paper) then the X-ray directional measurement $p^{\theta\theta}$ over three great circles can specify the solenoidal component or the directional Radon projections $r^{\alpha\alpha}$, $r^{\beta\beta}$ and directional X-ray projections $p^{\theta\theta}$ over one great circle together can specify the solenoidal component. This is ideal for an MRI experiment since cross terms are not required which cannot be obtained directly in an single scan [19]. Whereas, cross terms are required for reconstructing the irrotational component. Therefore, the knowledge that the tensor field is totally solenoidal can be important *a priori* information.

Expressing the decomposition in terms of scalar tensor and scalar vector potentials gives some flexibility in how algorithms are implemented. Analytical algorithms can be implemented to reconstruct the potential functions, from which the tensor field is determined by performing appropriate derivative operations, or the tensor field can be determined directly. In the case of the tensor potential we found that singularities existed in the implementation of the filter function. However, these same singularities did not exist if the solenoidal component of the tensor field was reconstructed directly.

A **cardiac diffusion tensor field** was chosen in our simulations to investigate the potential

application to MRI cardiac diffusion-tensor imaging. Our aim is to use MRI diffusion-tensor imaging to determine the fiber bundle orientation [2]-[5] in the myocardium from which one can specify a material axis for mechanical models [9]- [13] and identify conductive pathways [15] in order to develop electrical models of the heart. Thirty years ago Streeter and his colleagues quantified systematically the helical myocardial fiber structure [57]-[60] and more recent studies have been performed to do the same [63]-[65]. Comparison of diffusion-tensor MRI and histologic studies have shown that the principal eigenvector is nearly parallel to the fiber orientation in myocardial tissue [61], [62].

The **model of the heart muscle mechanics** is based on the passive and active behavior of skeletal muscle [9]-[13], in which the muscle is described by a quasi-incompressible transversely isotropic hyperelastic material [9], [66], [67]. The transversely isotropic material is defined relative to fiber bundle sheaths of a specified helical orientation in a manner similar to those used for skeletal muscle [66], [67]. Not only can MRI provide this structural information about fiber orientation (from diffusion tensor imaging) needed for the development of mechanical models, but it can also provide *in vivo* strain measurements [6]-[8] that can be compared to strain calculations obtained from the model. The characterization of cardiac deformation through strain measurements is an important part of the process of determining cardiac viability [68], quantifying ischemic injury, and evaluating perfusion by correlating perfusion with measures of strain [69].

The specification of cardiac diffusion tensor fields could also have potential application is the reconstruction of **conductivity tensor fields** in biological tissue [15]. This would be useful in the specification of the forward problems in solving the inverse MCG problem [70].

Tensor tomography could also have important application in **brain**. Already diffusion-tensor MRI is becoming an important application in the diagnosis of several brain disorders with the primary application in the diagnosis of acute stroke and ischemia [71]-[74]. It has also been found to be useful in diagnosing several other disorders. One of the most recent developments is the mapping of axon tracts in white matter for better characterization of white matter disease, as well as determining the correlation between function and morphology [75], [76], determining the

correlation between activation and white matter connectivity [77], [78], for surgical planning, and for the study of remodeling of function following brain injury [79].

Therefore, extensive work has already been accomplished in developing techniques for measuring diffusion tensor fields using MRI **without computed tomography**. The question is, will tensor computed tomography provide a more accurate and more efficient method for obtaining distributions of diffusion tensors in tissue, using MRI? The approach that is being proposed in this paper needs to be compared with these established MRI techniques as well as with new approaches that are presently being pursued. In one new approach [16], projections are formed of diffusion weighted MR images (not projections of the tensor field as we are proposing here). These projections are reconstructed to form diffusion-weighted images. With the application of different diffusion gradient weights, the spatial distribution of the diffusion tensor can be calculated. In the approach being proposed here, it has been shown that in order to form the projections of the diffusion tensor field, a linear approximation of the exponential attenuator in the expression for the diffusion-weighted signal must be made [19]. Also, manipulations of measurements need to be made in order to obtain desired scalar projection measurements of the diffusion tensor field. The reconstruction of the projections yields a spin density weighted diffusion tensor field. It is necessary to divide this by the reconstruction of the spin density to obtain the actual diffusion tensor field. Work still must be performed to verify whether this more indirect approach is more accurate than approaches that use conventional spin warp imaging or that use new tomographic techniques. It is possible that MRI tensor tomography is more efficient and less sensitive to strain modulation than methods previously proposed for imaging of diffusion tensor fields in the heart [2]-[5].

The results here may have application in **other areas of medical imaging** as well. For example, tensor tomography may be useful for in vivo mapping of cardiac deformation as it may provide a technique to obtain three-dimensional distributions of strain and stress tensor fields in the myocardium. It is interesting to note that various non-tomographic techniques using MRI have already made significant advancements towards being able to obtain three-dimensional strain maps of the myocardium [80]-[84]. Presently, one question must be answered before

tensor tomography can be applied to this problem: Can projections of strain and stress tensor fields be measured with a particular imaging modality?

In **summary**, tensor tomography builds upon the significant amount of work performed over the last ten years in vector tomography. The continuation of work in this area offers the potential for significant new mathematical developments in the field of inverse problems. The development of new algorithms in tensor tomography may have important application to *in vivo* mapping of brain diffusion tensors and cardiac strain, stress, diffusion, and conductivity tensors using MRI. Also, there is the potential for application to other imaging modalities that use acoustic or electrical magnetic radiation to measure tensor quantities in biological tissues. Information about the diffusion tensor field in the myocardium has direct application to both modeling of the mechanical properties, which are defined relative to the fiber bundle position and orientation in the heart which can be determined from a map of the diffusion tensor field, and to electrical conductivity properties in the heart which can also be inferred from the diffusion tensor field. These aspects of tensor tomography present fascinating areas of potential new research. Most certainly the advent of tensor tomography has created a rich arena for mathematical development.

ACKNOWLEDGEMENTS

This work was supported by the Benning Trust Fund. The authors would like to thank Sean Webb for carefully proofreading the manuscript.

APPENDIX I (Two-Dimensional Reconstruction of Tensor Fields)

The projection of a two-dimensional tensor field is

$$P(u;\theta)=\int_{-\infty}^{\infty}\theta^{T}T\left(t\underline{\theta}^{\perp}+u\underline{\theta}\right)\theta\,dt \quad , \tag{A1}$$

where

$$\theta=\begin{bmatrix}\cos\theta & -\sin\theta\\ \sin\theta & \cos\theta\end{bmatrix} \quad , \tag{A2}$$

and the columns of the matrix are the two vectors:

$$\underline{\theta}=(\cos\theta,\sin\theta) \quad , \tag{A3}$$

and

$$\underline{\theta}^{\perp}=(-\sin\theta,\cos\theta) \quad . \tag{A4}$$

The elements of the matrix P are

$$P(u;\theta)=\begin{bmatrix}p^{\theta\theta}(u;\theta) & p^{\theta\theta^{\perp}}(u;\theta)\\ p^{\theta^{\perp}\theta}(u;\theta) & p^{\theta^{\perp}\theta^{\perp}}(u;\theta)\end{bmatrix} \quad . \tag{A5}$$

The central section theorem is

$$\tilde{P}(v;\theta)=\theta^{T}\tilde{T}(v\underline{\theta})\theta \quad . \tag{A6}$$

We will consider the following decomposition of the two-dimensional tensor field *T*:

$$T(\underline{x})=T_{\Psi}^{S}(\underline{x})+T_{\Phi}^{I}(\underline{x}) \quad , \tag{A7}$$

where

$$\Psi(\underline{x})=\begin{bmatrix}0 & 0 & 0\\ 0 & 0 & 0\\ \dfrac{\partial X}{\partial y} & -\dfrac{\partial X}{\partial x} & 0\end{bmatrix} \quad , \tag{A8}$$

$$\Phi(\underline{x})=\begin{bmatrix}\Phi_1\\ \Phi_2\\ 0\end{bmatrix}(\underline{x}) \quad , \tag{A9}$$

result in

$$T^S_{\Psi}(\underline{x})=\nabla\times\Psi(\underline{x})=\begin{bmatrix}\frac{\partial^2 X}{\partial y^2} & -\frac{\partial^2 X}{\partial x\partial y}\\ -\frac{\partial^2 X}{\partial x\partial y} & \frac{\partial^2 X}{\partial x^2}\end{bmatrix} , \tag{A10}$$

$$T^I_{\Phi}(\underline{x})=\nabla\Phi(\underline{x})+[\nabla\Phi(\underline{x})]^T \quad , \tag{A11}$$

or

$$T^I_{\Phi}(\underline{x})=\nabla\Phi(\underline{x})=\begin{bmatrix}2\frac{\partial\Phi_x(\underline{x})}{\partial x} & \frac{\partial\Phi_y(\underline{x})}{\partial x}+\frac{\partial\Phi_x(\underline{x})}{\partial y}\\ \frac{\partial\Phi_y(\underline{x})}{\partial x}+\frac{\partial\Phi_x(\underline{x})}{\partial y} & 2\frac{\partial\Phi_y(\underline{x})}{\partial y}\end{bmatrix} . \tag{A12}$$

Now the Fourier transform of the tensor field decomposition give

$$\widetilde{T}(\underline{v})=2\pi i\begin{bmatrix}v_y^2\widetilde{X}(\underline{v}) & -v_xv_y\widetilde{X}(\underline{v})\\ -v_xv_y\widetilde{X}(\underline{v}) & v_x^2\widetilde{X}(\underline{v})\end{bmatrix}+2\pi i\begin{bmatrix}2v_x\widetilde{\Phi}_x(\underline{v}) & v_x\widetilde{\Phi}_y(\underline{v})+v_y\widetilde{\Phi}_x(\underline{v})\\ v_x\widetilde{\Phi}_y(\underline{v})+v_y\widetilde{\Phi}_x(\underline{v}) & 2v_y\widetilde{\Phi}_y(\underline{v})\end{bmatrix} . \tag{A13}$$

From the central section theorem, we know that

$$\widetilde{P}(\sigma;\theta)=\begin{bmatrix}\widetilde{p}^{\theta\theta}(\sigma;\theta) & \widetilde{p}^{\theta\theta^{\perp}}(\sigma;\theta)\\ \widetilde{p}^{\theta^{\perp}\theta}(\sigma;\theta) & \widetilde{p}^{\theta^{\perp}\theta^{\perp}}(\sigma;\theta)\end{bmatrix}=\theta^T\widetilde{T}(\sigma\,\underline{\theta})\theta \quad . \tag{A14}$$

Substituting the decomposition for T, we have

$$\begin{bmatrix} \widetilde{p}^{\theta\theta}(\sigma;\theta) & \widetilde{p}^{\theta\theta'}(\sigma;\theta) \\ \widetilde{p}^{\theta'\theta}(\sigma;\theta) & \widetilde{p}^{\theta'\theta'}(\sigma;\theta) \end{bmatrix} = 2\pi i\theta^T \begin{bmatrix} \sigma^2 \sin^2\theta\, \widetilde{X}(\sigma\underline{\theta}) & -\sigma^2 \sin\theta\cos\theta\, \widetilde{X}(\sigma\underline{\theta}) \\ -\sigma^2 \sin\theta\cos\theta\, \widetilde{X}(\sigma\underline{\theta}) & \sigma^2 \cos^2\theta\, \widetilde{X}(\sigma\underline{\theta}) \end{bmatrix} \theta$$

$$+2\pi i\theta^T \begin{bmatrix} 2\sigma\cos\theta\, \widetilde{\Phi}_x(\sigma\underline{\theta}) & \sigma\cos\theta\, \widetilde{\Phi}_y(\sigma\underline{\theta}) + \sigma\sin\theta\, \widetilde{\Phi}_x(\sigma\underline{\theta}) \\ \sigma\cos\theta\, \widetilde{\Phi}_y(\sigma\underline{\theta}) + \sigma\sin\theta\, \widetilde{\Phi}_x(\sigma\underline{\theta}) & 2\sigma\sin\theta\, \widetilde{\Phi}_y(\sigma\underline{\theta}) \end{bmatrix} \theta$$

(A15)

$$\begin{bmatrix} \widetilde{p}^{\theta\theta}(\sigma;\theta) & \widetilde{p}^{\theta\theta'}(\sigma;\theta) \\ \widetilde{p}^{\theta\theta'}(\sigma;\theta) & \widetilde{p}^{\theta'\theta'}(\sigma;\theta) \end{bmatrix} = 2\pi i \begin{bmatrix} 0 & 0 \\ 0 & \sigma^2 \widetilde{X}(\sigma\underline{\theta}) \end{bmatrix}$$

$$+2\pi i \begin{bmatrix} 2\sigma(\cos\theta\, \widetilde{\Phi}_x(\sigma\underline{\theta}) + \sin\theta\, \widetilde{\Phi}_y(\sigma\underline{\theta})) & -\sigma\sin\theta\, \widetilde{\Phi}_x(\sigma\underline{\theta}) + \sigma\cos\theta\, \widetilde{\Phi}_y(\sigma\underline{\theta}) \\ -\sigma\sin\theta\, \widetilde{\Phi}_x(\sigma\underline{\theta}) + \sigma\cos\theta\, \widetilde{\Phi}_y(\sigma\underline{\theta}) & 0 \end{bmatrix}$$

(A16)

Note that $p^{\theta'\theta'}(u;\theta)$ will determine the solenodial component and $p^{\theta\theta}(u;\theta)$ and $p^{\theta\theta'}(u;\theta)$ will determine the irrotational component of the tensor field decomposition.

APPENDIX II (X-ray Transform)

From equation (34), we have the Fourier transform of the X-ray projections given by

$$\widetilde{P}\left(v_u, v_v; \underline{\theta}\right)=\begin{bmatrix} \widetilde{p}^{\theta\theta} & \widetilde{p}^{\theta\alpha} & \widetilde{p}^{\theta\beta} \\ \widetilde{p}^{\alpha\theta} & \widetilde{p}^{\alpha\alpha} & \widetilde{p}^{\alpha\beta} \\ \widetilde{p}^{\beta\theta} & \widetilde{p}^{\beta\alpha} & \widetilde{p}^{\beta\beta} \end{bmatrix}\left(v_u, v_v; \underline{\theta}\right)=\theta^T \widetilde{T}^S_\Psi\left(v_u \underline{\alpha}+v_v \underline{\beta}\right)\theta+\theta^T \widetilde{T}^I_\Phi\left(v_u \underline{\alpha}+v_v \underline{\beta}\right)\theta \tag{B1}$$

For the **solenoid** term, we have

$$\theta^T \widetilde{T}^S_\Psi\left(v_u \underline{\alpha}+v_v \underline{\beta}\right)\theta=$$

$$2\pi i\theta^T\left[\left(v_u \underline{\alpha}+v_v \underline{\beta}\right)\times\widetilde{\Psi}\left(v_u \underline{\alpha}+v_v \underline{\beta}\right)\right]\theta=2\pi i\begin{bmatrix} \left(\theta^T \widetilde{T}^S_\Psi \theta\right)_{\theta\theta} & \left(\theta^T \widetilde{T}^S_\Psi \theta\right)_{\theta\alpha} & \left(\theta^T \widetilde{T}^S_\Psi \theta\right)_{\theta\beta} \\ \left(\theta^T \widetilde{T}^S_\Psi \theta\right)_{\alpha\theta} & \left(\theta^T \widetilde{T}^S_\Psi \theta\right)_{\alpha\alpha} & \left(\theta^T \widetilde{T}^S_\Psi \theta\right)_{\alpha\beta} \\ \left(\theta^T \widetilde{T}^S_\Psi \theta\right)_{\beta\theta} & \left(\theta^T \widetilde{T}^S_\Psi \theta\right)_{\beta\alpha} & \left(\theta^T \widetilde{T}^S_\Psi \theta\right)_{\beta\beta} \end{bmatrix}\left(v_u \underline{\alpha}+v_v \underline{\beta}\right) \tag{B2}$$

where

¿¿ ¿ ¿¿ (B3)

¿¿ ¿ ¿¿+sin(¿2θ)$v_u v_v \widetilde{X}_3\left(v_u \underline{\alpha}+v_v \underline{\beta}\right)$¿ (B4)

¿¿ ¿ ¿¿−sin(¿2θ)$v_u^2 \widetilde{X}_3\left(v_u \underline{\alpha}+v_v \underline{\beta}\right)$¿ (B5)

¿¿ ¿ ¿¿+sin(¿2θ)$v_u v_v \widetilde{X}_3\left(v_u \underline{\alpha}+v_v \underline{\beta}\right)$¿ (B6)

¿+cos²(¿θ)$v_v^2 \widetilde{X}_3\left(v_u \underline{\alpha}+v_v \underline{\beta}\right)$¿ (B7)

¿¿ ¿ ¿ (B8)

¿¿ ¿ ¿¿−sin(¿2θ)$v_u^2 \widetilde{X}_3\left(v_u \underline{\alpha}+v_v \underline{\beta}\right)$¿ (B9)

¿¿ ¿ ¿ (B10)

and

¿¿ ¿ ¿ . (B11)

For the **irrotational** term, we have

$$\theta^T \tilde{T}^I_{\Phi}\left(v_u \underline{\alpha}+v_v \underline{\beta}\right)\theta=$$

$$2\pi i\theta^T\left\{\left(v_u \underline{\alpha}+v_v \underline{\beta}\right)\tilde{\Phi}\left(v_u \underline{\alpha}+v_v \underline{\beta}\right)+\left[\left(v_u \underline{\alpha}+v_v \underline{\beta}\right)\tilde{\Phi}\left(v_u \underline{\alpha}+v_v \underline{\beta}\right)\right]^T\right\}\theta$$

$$=2\pi i\begin{bmatrix}\left(\theta^T \tilde{T}^I_{\Phi}\theta\right)_{\theta\theta} & \left(\theta^T \tilde{T}^I_{\Phi}\theta\right)_{\theta\alpha} & \left(\theta^T \tilde{T}^I_{\Phi}\theta\right)_{\theta\beta}\\ \left(\theta^T \tilde{T}^I_{\Phi}\theta\right)_{\alpha\theta} & \left(\theta^T \tilde{T}^I_{\Phi}\theta\right)_{\alpha\alpha} & \left(\theta^T \tilde{T}^I_{\Phi}\theta\right)_{\alpha\beta}\\ \left(\theta^T \tilde{T}^I_{\Phi}\theta\right)_{\beta\theta} & \left(\theta^T \tilde{T}^I_{\Phi}\theta\right)_{\beta\alpha} & \left(\theta^T \tilde{T}^I_{\Phi}\theta\right)_{\beta\beta}\end{bmatrix}\left(v_u \underline{\alpha}+v_v \underline{\beta}\right) \tag{B12}$$

where

$$\left(\theta^T \tilde{T}^I_{\Phi}\theta\right)_{\theta\theta}\left(v_u \underline{\alpha}+v_v \underline{\beta}\right)=0 \tag{B13}$$

$$\begin{aligned}\left(\theta^T \tilde{T}^I_{\Phi}\theta\right)_{\theta\alpha}\left(v_u \underline{\alpha}+v_v \underline{\beta}\right)&=v_u\cos(\varphi)\sin(\theta)\tilde{\Phi}_1\left(v_u \underline{\alpha}+v_v \underline{\beta}\right)\\&+v_u\sin(\theta)\sin(\varphi)\tilde{\Phi}_2\left(v_u \underline{\alpha}+v_v \underline{\beta}\right)\\&+v_u\cos(\theta)\tilde{\Phi}_3\left(v_u \underline{\alpha}+v_v \underline{\beta}\right)\end{aligned} \tag{B14}$$

$$\begin{aligned}\left(\theta^T \tilde{T}^I_{\Phi}\theta\right)_{\theta\beta}\left(v_u \underline{\alpha}+v_v \underline{\beta}\right)&=v_v\cos(\varphi)\sin(\theta)\tilde{\Phi}_1\left(v_u \underline{\alpha}+v_v \underline{\beta}\right)\\&+v_v\sin(\theta)\sin(\varphi)\tilde{\Phi}_2\left(v_u \underline{\alpha}+v_v \underline{\beta}\right)\\&+v_v\cos(\theta)\tilde{\Phi}_3\left(v_u \underline{\alpha}+v_v \underline{\beta}\right)\end{aligned} \tag{B15}$$

$$\begin{aligned}\left(\theta^T \tilde{T}^I_{\Phi}\theta\right)_{\alpha\theta}\left(v_u \underline{\alpha}+v_v \underline{\beta}\right)&=v_u\cos(\varphi)\sin(\theta)\tilde{\Phi}_1\left(v_u \underline{\alpha}+v_v \underline{\theta}\right)\\&+v_u\sin(\theta)\sin(\varphi)\tilde{\Phi}_2\left(v_u \underline{\alpha}+v_v \underline{\theta}\right)\\&+v_u\cos(\theta)\tilde{\Phi}_3\left(v_u \underline{\alpha}+v_v \underline{\theta}\right)\end{aligned} \tag{B16}$$

$$\left(\theta^T \tilde{T}^I_{\Phi}\theta\right)_{\alpha\alpha}\left(v_u \underline{\alpha}+v_v \underline{\beta}\right)=-2v_u\sin(\varphi)\tilde{\Phi}_1\left(v_u \underline{\alpha}+v_v \underline{\beta}\right)+2v_u\cos(\varphi)\tilde{\Phi}_2\left(v_u \underline{\alpha}+v_v \underline{\beta}\right) \tag{B17}$$

$$\begin{aligned}\left(\theta^T \tilde{T}^I_{\Phi}\theta\right)_{\alpha\beta}\left(v_u \underline{\alpha}+v_v \underline{\beta}\right)&=-\left(v_v\sin(\varphi)+v_u\cos(\theta)\cos(\varphi)\right)\tilde{\Phi}_1\left(v_u \underline{\alpha}+v_v \underline{\beta}\right)\\&-\left(v_u\cos(\theta)\sin(\varphi)-v_v\cos(\varphi)\right)\tilde{\Phi}_2\left(v_u \underline{\alpha}+v_v \underline{\beta}\right)\\&+\sin(\theta)v_u\tilde{\Phi}_3\left(v_u \underline{\alpha}+v_v \underline{\beta}\right)\end{aligned} \tag{B18}$$

$$\left(\theta^T \tilde{T}^I_{\Phi} \theta\right)_{\beta\theta}\left(v_u \underline{\alpha} + v_v \underline{\beta}\right) = v_v \cos(\varphi)\sin(\theta)\tilde{\Phi}_1\left(v_u \underline{\alpha} + v_v \underline{\beta}\right) + v_v \sin(\theta)\sin(\varphi)\tilde{\Phi}_2\left(v_u \underline{\alpha} + v_v \underline{\beta}\right) + v_v \cos(\theta)\tilde{\Phi}_3\left(v_u \underline{\alpha} + v_v \underline{\beta}\right) \quad \text{(B19)}$$

$$\left(\theta^T \tilde{T}^I_{\Phi} \theta\right)_{\beta\alpha}\left(v_u \underline{\alpha} + v_v \underline{\beta}\right) = -\left(v_v \sin(\varphi) + v_u \cos(\theta)\cos(\varphi)\right)\tilde{\Phi}_1\left(v_u \underline{\alpha} + v_v \underline{\beta}\right) - \left(v_u \cos(\theta)\sin(\varphi) - v_v \cos(\varphi)\right)\tilde{\Phi}_2\left(v_u \underline{\alpha} + v_v \underline{\beta}\right) + \sin(\theta) v_u \tilde{\Phi}_3\left(v_u \underline{\alpha} + v_v \underline{\beta}\right) \quad \text{(B20)}$$

and

$$\left(\theta^T \tilde{T}^I_{\Phi} \theta\right)_{\beta\beta}\left(v_u \underline{\alpha} + v_v \underline{\beta}\right) = -2 v_v \cos(\theta)\cos(\varphi)\tilde{\Phi}_1\left(v_u \underline{\alpha} + v_v \underline{\beta}\right) - 2 v_v \cos(\theta)\sin(\varphi)\tilde{\Phi}_2\left(v_u \underline{\alpha} + v_v \underline{\beta}\right)\right) + 2 v_v \sin(\theta)\tilde{\Phi}_3\left(v_u \underline{\alpha} + v_v \underline{\beta}\right) \quad . \quad \text{(B21)}$$

Therefore,

$$\tilde{P}\left(v_u, v_v; \underline{\theta}\right) = \begin{bmatrix} \tilde{p}^{\theta\theta} & \tilde{p}^{\theta\alpha} & \tilde{p}^{\theta\beta} \\ \tilde{p}^{\alpha\theta} & \tilde{p}^{\alpha\alpha} & \tilde{p}^{\alpha\beta} \\ \tilde{p}^{\beta\theta} & \tilde{p}^{\beta\alpha} & \tilde{p}^{\beta\beta} \end{bmatrix}\left(v_u, v_v; \underline{\theta}\right) = \begin{bmatrix} X & X & X \\ X & X & X \\ X & X & X \end{bmatrix} + \begin{bmatrix} 0 & X & X \\ X & X & X \\ X & X & X \end{bmatrix} . \quad \text{(B22)}$$

APPENDIX III (Radon Transform)

From equation (39), we have the Fourier transform of the Radon projections given by

$$\widetilde{R}(v_t;\underline{\theta})=\begin{bmatrix}\widetilde{r}^{\theta\theta} & \widetilde{r}^{\theta\alpha} & \widetilde{r}^{\theta\beta}\\ \widetilde{r}^{\alpha\theta} & \widetilde{r}^{\alpha\alpha} & \widetilde{r}^{\alpha\beta}\\ \widetilde{r}^{\beta\theta} & \widetilde{r}^{\beta\alpha} & \widetilde{r}^{\beta\beta}\end{bmatrix}(v_t;\underline{\theta})=\theta^T\widetilde{T}^S_\Psi(v_t\underline{\theta})\theta+\theta^T\widetilde{T}^I_\Phi(v_t\underline{\theta})\theta \quad . \qquad \text{(C1)}$$

For the **solenoid** component, we have

$$\theta^T\widetilde{T}^S_\Psi(v_t\underline{\theta})\theta=2\pi i\theta^T[(v_t\underline{\theta})\times\widetilde{\Psi}(v_t\underline{\theta})]\theta$$

$$=2\pi i\begin{bmatrix}(\theta^T\widetilde{T}^S_\Psi\theta)_{\theta\theta} & (\theta^T\widetilde{T}^S_\Psi\theta)_{\theta\alpha} & (\theta^T\widetilde{T}^S_\Psi\theta)_{\theta\beta}\\ (\theta^T\widetilde{T}^S_\Psi\theta)_{\alpha\theta} & (\theta^T\widetilde{T}^S_\Psi\theta)_{\alpha\alpha} & (\theta^T\widetilde{T}^S_\Psi\theta)_{\alpha\beta}\\ (\theta^T\widetilde{T}^S_\Psi\theta)_{\beta\theta} & (\theta^T\widetilde{T}^S_\Psi\theta)_{\beta\alpha} & (\theta^T\widetilde{T}^S_\Psi\theta)_{\beta\beta}\end{bmatrix}(v_t\underline{\theta}) \qquad \text{(C2)}$$

where

$$(\theta^T\widetilde{T}^S_\Psi\theta)_{\theta\theta}(v_t\underline{\theta})=0 \qquad \text{(C3)}$$

$$(\theta^T\widetilde{T}^S_\Psi\theta)_{\theta\alpha}(v_t\underline{\theta})=0 \qquad \text{(C4)}$$

$$(\theta^T\widetilde{T}^S_\Psi\theta)_{\theta\beta}(v_t\underline{\theta})=0 \qquad \text{(C5)}$$

$$(\theta^T\widetilde{T}^S_\Psi\theta)_{\alpha\theta}(v_t\underline{\theta})=0 \qquad \text{(C6)}$$

$$(\theta^T\widetilde{T}^S_\Psi\theta)_{\alpha\alpha}(v_t\underline{\theta})=v_t^2\cos^2(\theta)\cos^2(\varphi)\widetilde{X}_1(v_t\underline{\theta})+v_t^2\cos^2(\theta)\sin^2(\varphi)\widetilde{X}_2(v_t\underline{\theta})+v_t^2\sin^2(\theta)\widetilde{X}_3(v_t\underline{\theta}) \qquad \text{(C7)}$$

$$(\theta^T\widetilde{T}^S_\Psi\theta)_{\alpha\beta}(v_t\underline{\theta})=-\frac{1}{2}v_t^2\cos(\theta)\sin(2\varphi)\widetilde{X}_1(v_t\underline{\theta})+\frac{1}{2}v_t^2\cos(\theta)\sin(2\varphi)\widetilde{X}_2(v_t\underline{\theta}) \qquad \text{(C8)}$$

$$(\theta^T\widetilde{T}^S_\Psi\theta)_{\beta\theta}(v_t\underline{\theta})=0 \qquad \text{(C9)}$$

$$(\theta^T\widetilde{T}^S_\Psi\theta)_{\beta\alpha}(v_t\underline{\theta})=-\frac{1}{2}v_t^2\cos^2(\theta)\sin(2\varphi)\widetilde{X}_1(v_t\underline{\theta})+\frac{1}{2}v_t^2\cos^2(\theta)\sin(2\varphi)\widetilde{X}_2(v_t\underline{\theta}) \qquad \text{(C10)}$$

$$\left(\theta^T \tilde{T}^S_{\Psi} \theta\right)_{\beta\beta}\left(v_t \underline{\theta}\right) = v_t^2 \sin^2(\varphi)\tilde{X}_1\left(v_t \underline{\theta}\right) + v_t^2 \cos^2(\varphi)\tilde{X}_2\left(v_t \underline{\theta}\right) \quad . \tag{C11}$$

For the **irrotational** component, we have

$$\theta^T \tilde{T}^I_{\Phi}\left(v_t \underline{\theta}\right)\theta = 2\pi i \theta^T \left\{\left(v_t \underline{\theta}\right)\tilde{\Phi}\left(v_t \underline{\theta}\right) + \left[\left(v_t \underline{\theta}\right)\tilde{\Phi}\left(v_t \underline{\theta}\right)\right]^T\right\}\theta$$

$$= 2\pi i \begin{bmatrix} \left(\theta^T \tilde{T}^I_{\Phi}\theta\right)_{\theta\theta} & \left(\theta^T \tilde{T}^I_{\Phi}\theta\right)_{\theta\alpha} & \left(\theta^T \tilde{T}^I_{\Phi}\theta\right)_{\theta\beta} \\ \left(\theta^T \tilde{T}^I_{\Phi}\theta\right)_{\alpha\theta} & \left(\theta^T \tilde{T}^I_{\Phi}\theta\right)_{\alpha\alpha} & \left(\theta^T \tilde{T}^I_{\Phi}\theta\right)_{\alpha\beta} \\ \left(\theta^T \tilde{T}^I_{\Phi}\theta\right)_{\beta\theta} & \left(\theta^T \tilde{T}^I_{\Phi}\theta\right)_{\beta\alpha} & \left(\theta^T \tilde{T}^I_{\Phi}\theta\right)_{\beta\beta} \end{bmatrix}\left(v_t \underline{\theta}\right) \tag{C12}$$

where

$$\left(\theta^T \tilde{T}^I_{\Phi}\theta\right)_{\theta\theta}\left(v_t \underline{\theta}\right) = 2 v_t \cos(\varphi)\sin(\theta)\tilde{\Phi}_1\left(v_t \underline{\theta}\right) + 2 v_t \sin(\theta)\sin(\varphi)\tilde{\Phi}_2\left(v_t \underline{\theta}\right) + 2 v_t \cos(\theta)\tilde{\Phi}_3\left(v_t \underline{\theta}\right) \tag{C13}$$

$$\left(\theta^T \tilde{T}^I_{\Phi}\theta\right)_{\theta\alpha}\left(v_t \underline{\theta}\right) = -v_t \sin(\varphi)\tilde{\Phi}_1\left(v_t \underline{\theta}\right) + v_t \cos(\varphi)\tilde{\Phi}_2\left(v_t \underline{\theta}\right) \tag{C14}$$

$$\left(\theta^T \tilde{T}^I_{\Phi}\theta\right)_{\theta\beta}\left(v_t \underline{\theta}\right) = -v_t \cos(\theta)\cos(\varphi)\tilde{\Phi}_1\left(v_t \underline{\theta}\right) - v_t \cos(\theta)\sin(\varphi)\tilde{\Phi}_2\left(v_t \underline{\theta}\right) + v_t \sin(\theta)\tilde{\Phi}_3\left(v_t \underline{\theta}\right) \tag{C15}$$

$$\left(\theta^T \tilde{T}^I_{\Phi}\theta\right)_{\alpha\theta}\left(v_t \underline{\theta}\right) = -v_t \sin(\varphi)\tilde{\Phi}_1\left(v_t \underline{\theta}\right) + v_t \cos(\varphi)\tilde{\Phi}_2\left(v_t \underline{\theta}\right) \tag{C16}$$

$$\left(\theta^T \tilde{T}^I_{\Phi}\theta\right)_{\alpha\alpha}\left(v_t \underline{\theta}\right) = 0 \tag{C17}$$

$$\left(\theta^T \tilde{T}^I_{\Phi}\theta\right)_{\alpha\beta}\left(v_t \underline{\theta}\right) = 0 \tag{C18}$$

$$\left(\theta^T \tilde{T}^I_{\Phi}\theta\right)_{\beta\theta}\left(v_t \underline{\theta}\right) = -v_t \cos(\theta)\cos(\varphi)\tilde{\Phi}_1\left(v_t \underline{\theta}\right) - v_t \cos(\theta)\sin(\varphi)\tilde{\Phi}_2\left(v_t \underline{\theta}\right) + v_t \sin(\theta)\tilde{\Phi}_3\left(v_t \underline{\theta}\right) \tag{C19}$$

$$\left(\theta^T \tilde{T}^I_{\Phi}\theta\right)_{\beta\alpha}\left(v_t \underline{\theta}\right) = 0 \tag{C20}$$

$$\left(\theta^T \tilde{T}^I_{\Phi}\theta\right)_{\beta\beta}\left(v_t \underline{\theta}\right) = 0 \tag{C21}$$

and,

$$\widetilde{R}(v_t;\underline{\theta})=\begin{bmatrix}\widetilde{r}^{\theta\theta} & \widetilde{r}^{\theta\alpha} & \widetilde{r}^{\theta\beta}\\ \widetilde{r}^{\alpha\theta} & \widetilde{r}^{\alpha\alpha} & \widetilde{r}^{\alpha\beta}\\ \widetilde{r}^{\beta\theta} & \widetilde{r}^{\beta\alpha} & \widetilde{r}^{\beta\beta}\end{bmatrix}(v_t;\underline{\theta})=\begin{bmatrix}0 & 0 & 0\\ 0 & X & X\\ 0 & X & X\end{bmatrix}+\begin{bmatrix}X & X & X\\ X & 0 & 0\\ X & 0 & 0\end{bmatrix}. \qquad \text{(C22)}$$

REFERENCES

[1] C. Pierpaoli, P. Jezzard, P. J. Barnett, *et al.*, "Diffusion tensor MR imaging of the human brain," *Radiology*, vol. 201, pp. 637-648, 1999.

[2] R. R. Edelman, J. Gaa, V. J. Wedeen, E. Loh, J. M. Hare, P. Prasad, W. Li, "In vivo measurement of water diffusion in the human heart," *Magn. Reson. Med.*, vol. 32, pp. 423-428, 1994.

[3] T. G. Reese, R. M. Weisskoff, R. N. Smith, B. R. Rosen, R. E. Dinsmore, and V. J. Wedeen, "Imaging myocardial fiber architecture in vivo with magnetic resonance," *Magn. Reson. Med.*, vol. 34, pp. 786-791, 1995.

[4] T. G. Reese, V. J. Wedeen, and R. M. Weisskoff, "Measuring diffusion in the presence of material strain," *J. Magn. Reson. B*, vol. 112, pp. 253-258, 1996.

[5] W.Y. Tseng, T. G. Resse, and R. M. Weisskoff, V. J. Wedeen: "Cardiac diffusion tensor MRI in vivo without strain correction," *Magn. Reson. Med.*, vol. 42, pp. 393-403, 1999.

[6] V. J. Wedeen, "Magnetic resonance imaging of myocardial kinematics. Technique to detect, localize, and quantify the strain rates of the active human myocardium," *J. Magn. Reson. Imag.*, vol. 2, pp. 575-582, 1992.

[7] V. J. Wedeen, R. M. Weisskoff, T. G. Resse, G. M. Beache, B. P. Poncelet, B. R. Rosen, and R. E. Dinsmore, "Motionless movies of myocardial strain rates using stimulated echoes," *Magn. Reson. Med.*, vol. 33, pp. 401-408, 1995.

[8] M. D. Robson and R. T. Constable, "Three-dimensional strain-rate imaging," *Magn. Reson. Med.*, vol. 36, pp. 537-546, 1996.

[9] J. M. Guccione, A. D. McCulloch, and L. K. Waldman, "Passive material properties of intact ventricular myocardium determined from a cylindrical model," *Trans. of the ASME*, vol. 113, pp. 42-55, 1991.

[10] J. M. Guccione and A. D. McCulloch, "Mechanics of active contraction in cardiac muscle: Part I – Constitutive relations for fiber stress that describe deactivation," *Trans.*

of the ASME, vol. 115, pp. 72-81, 1993.

[11] J. M. Guccione, L. K. Waldman, and A. D. McCulloch, "Mechanics of active contraction in cardiac muscle: Part II – Cylindrical models of the systolic left ventricle, *Trans. of the ASME*, vol. 115, pp. 82-90, 1993.

[12] K. D. Costa, P. J. Hunter, J. M. Rogers, J. M. Guccione, L. K. Waldman, and A. D. McCulloch, "A three-dimensional finite element method for large elastic deformations of ventricular myocardium: I – Cylindrical and spherical polar coordinates," *Trans. of the ASME*, vol. 118, pp. 452-463, 1996.

[13] K. D. Costa, P. J. Hunter, J. M. Rogers, J. M. Guccione, L. K. Waldman, A. D. McCulloch, "A three-dimensional finite element method for large elastic deformations of ventricular myocardium: II – Prolate spheroidal coordinates," *Trans. of the ASME*, vol. 118, pp. 464-472, 1996.

[14] G. T. Gullberg, A. Sitek, E. V. R. Di Bella, B. Feng, P. E. Christian and W. D. Adams, "Mechanical modeling of the myocardium using gated SPECT," *J. Nucl. Cardiol.*, vol. 6, p. S116, 1999.

[15] D. S. Turch, V. J. Wedeen, A. M. Dale and J. W. Belliveau, "Electrical conductivity tensor map of the human brain using NMR diffusion imaging: An effective medium approach," in *Proceedings of the International Society for Magnetic Resonance in Medicine*, Sydney, Australia, April 18-24, p. 527, 1998.

[16] A. F. Gmitro and A. L. Alexander, "Use of a projection reconstruction method to decrease motion sensitivity in diffusion-weighted MRI," *Magn. Reson. Med.*, vol. 29, pp. 835-838, 1993.

[17] J. Mattiello, P. J. Basser and D. LeBihan, "Analytical expressions for the b matrix in NMR diffusion tensor imaging and spectroscopy," *J. Magn. Reson. A*, vol. 108, pp. 131-141, 1994.

[18] J. Mattiello, P. J. Basser and D. LeBihan, "The b matrix in diffusion tensor echo-planar

imaging," *Magn. Reson. Med.*, vol. 37, pp. 292-300, 1997.

[19] G. T. Gullberg, D. Ghosh Roy, G. L. Zeng, A. L. Alexander and D. L. Parker, "Tensor tomography," *IEEE Trans. on Nucl. Sci*., vol. 46, pp. 991-1000, 1999.

[20] J. L. Prince, "Convolution backprojection formulas for 3-D vector tomography with application to MRI," *IEEE Trans. on Image Processing*, vol. 5, pp. 1462-1472, 1996.

[21] S. A. Johnson, J. F. Greenleaf, M. Tanaka and G. Flandro, "Reconstructing three-dimensional fluid velocity vector fields from acoustic transmission measurements," in *Acoustical Holography*, Vol. 7, Ed: L. Kesler, Plenum, New York. 1977, pp. 307-326.

[22] G. Arfken, *Mathematical Methods for Physicists*, Academic Press, Inc., San Diego, 1985.

[23] S. Takuso, *et al.*, "Introduction of mass conversation law to improve the tomographic estimation of flow velocity distribution from differential time-of-flight data," *J. Acoust. Soc. Amer.*, vol. 77, pp. 2104-2106, 1985.

[24] W. Munk and C. Wunsch, "Ocean acoustic tomography: A scheme for large-scale monitoring," *Deep-Sea Research*, vol. 26A, pp. 123-161, 1979.

[25] B. M. Howe, P. F. Worchester and W. Munk, "Ocean acoustic tomography: Mesoscale velocity," *J. Geophys. Research*, vol. 92, pp. 3785-3805, 1987.

[26] S. J. Norton, "Tomographic reconstruction of 2-D vector fields: Application to flow imaging," *Geophys J.*, vol. 97, pp. 161-168, 1988.

[27] S. J. Norton, "Unique tomographic reconstruction of vector fields using boundary data," *IEEE Trans. on Image Processing*, vol. 1, pp. 406-412, 1992.

[28] D. M. Kramer and P. C. Lauterbur, "On the problem of reconstructing images of nonscalar parameters from projections. Application to vector fields," *IEEE Trans. on Nucl. Sci.*, vol. NS-26, pp. 2674-2677, 1979.

[29] K. B. Winters and D. Rouseff, "A filtered backprojection method for the tomographic reconstruction of fluid vorticity," *Inverse Problems*, vol. 6, pp. L33-L38, 1990.

[30] K. B. Winters and D. Rouseff, "Tomographic reconstruction of stratified fluid flow," *IEEE Trans. on Ultrasonics, Ferroelectrics and Frequency Control*, vol. 40, pp. 26-33, 1993.

[31] D. Rouseff, K. B. Winters and T. E. Ewart, "Reconstruction of oceanic microstructure by tomography: A numerical feasibility study," *J. Geophysical Research*, vol. 96, pp. 8823-8833, 1991.

[32] H. Braun and A. Hauck, "Tomographic reconstruction of vector fields," *IEEE Trans. on Signal Process.*, vol. 39, pp. 464-471, 1991.

[33] N. F. Osman and J. L. Prince, "3D vector tomography on bounded domains," *Inverse Problems*, vol. 14, pp. 185-196, 1998.

[34] G. W. Faris and R. L. Byer, "Three-dimensional beam-deflection optical tomography of a supersonic jet" *Applied Optics*, vol. 27, pp. 5202-5212, 1988.

[35] M. Zahn, "Transform relationship between Kerr-effect optical phase shift and non-uniform electrical field distributions," *Trans. on Dielectrics and Electrical Insulation*, vol. 1, pp. 235-246, 1994.

[36] Y. A. Andrienko, M. S. Duboikov and A. D. Gladun, "Optical tensor field tomography: the Kerr effect and axisymmetric integrated photoelasticity," *J. Opt. Soc. Am. A.*, vol. 9, pp. 1765-1768, 1992.

[37] V. A. Sharafutdinov, "Tomographic method in optics," in *Proceedings of SPIE: Tomographic Methods in Optics*, 1991.

[38] H. Aben, *Integrated Photoelasticity*, McGraw-Hill, Inc., New York, 1979.

[39] H. Aben and A. Puro, "Photoelastic tomography for three-dimensional flow birefringence studies," *Inverse Problems*, vol. 13, pp. 215-221, 1995.

[40] A. Schwarz, "Three-dimensional reconstruction of temperature and velocity fields in a furnace," in *Proceeding of ECAPT, The European Concerted Action on Process*

Tomography, pp. 227-233, 1994.

[41] N. Efremov, N. Pamentov and V. Kharachenko, "Tomography of ion and atom velocities in plasmas," *J. Quant. Spectrosc. Radiation Transfer*, vol. 6, pp. 723-728, 1995.

[42] P. Juhlin, "Doppler tomography," in *Proceedings of the 15th Annual International Conference of the IEEE Engineering in Medicine and Biology Society*, 1993.

[43] P. Juhlin, *Principles of Doppler Tomography*, Technical Report, Department of Mathematics, Lund Institute of Technology, 1992.

[44] K. Strahlen, *Some Integral Transforms of Vector Fields*, Licentiate Thesis, Department of Mathematics, Lund Institute of Technology, 1996.

[45] G. Sparr, K. Strahlen, K. Lindstrom and H. W. Persson, "Doppler tomography for vector fields," *Inverse Problems*, vol. 11, pp. 1051-1061, 1995.

[46] A. M. Denisov, A. A. Popov and V. V. Sterlyadkin, "Doppler tomography problem for a two-dimensional vector field*," Moscow University Computational Mathematics and Cybernetics*, vol. 1, pp. 17-20, 1995.

[47] L. Desbat and A. Wernsdorfer, "Direct algebraic reconstruction and optimal sampling in vector field tomography," *IEEE Trans. on Signal Processing*, vol. 43, pp. 1798-1808, 1995.

[48] L. Desbat, "Efficient parallel sampling in vector field tomography," *Inverse Problems*, vol. 11, pp. 995-1003, 1995.

[49] G. Sparr and K. Strahlen, "Vector field tomography, An overview," To appear in *IMA Volumes in Mathematics and its Applications; Computational Radiology and Imaging: Therapy and Diagnostics* (Springer Verlag).

[50] *Mathematics and Physics of Emerging Biomedical Imaging*, National Academy Press, Washington, D.C., 1996.

[51] V. A. Sharafutdinov, *Integral Geometry of Tensor Fields*, VSP, Utrecht, 1994.

[52] I. M. Gelfand, S. G. Gindikin and M. I. Graev, “Integral geometry in affine and projective spaces,” *J. Sov. Math.*, vol. 18, pp. 39-167, 1982.

[53] D. C. Kay, *Tensor Calculus*, Schaum's Outline Series in Mathematics, McGraw-Hill Book Company, 1988.

[54] B. Spain, *Tensor Calculus*, Oliver and Boyd, Edinburgh and London, New York: Interscience Publishers, Inc. 1956.

[55] A. J. McConnell, *Applications of Tensor Analysis*, Dover Publications, Inc., New York, 1957.

[56] J. R. Tyldesley, *An Introduction to Tensor Analysis for Engineers and Applied Scientists*, Longman Group Limited, London, 1975.

[57] D. D. Streeter and D. L. Bassett, “An engineering analysis of myocardial fiber orientation in a pig’s left ventricle in systole,” *Anat. Rec.*, vol. 155, pp. 503-511, 1966.

[58] D. D. Streeter, H. M. Spotnitz, P. Patel, J. Ross and E. H. Sonnenblick, “Fiber orientation in the canine left ventricle during systole and diastole,” *Circ. Res.*, vol. 24, pp. 339-347, 1969.

[59] D. D. Streeter and W. T. Hanna, “Engineering mechanics for successive states in canine left ventricular myocardium. I. Cavity and wall geometry,” *Circ. Res*., vol. 33, pp. 639-655, 1973.

[60] D. D. Streeter, “Gross morphology and fiber geometry of the heart,” *in Handbook of Physiology*, R. M. Berne, editor, Besthesda, MD, American Physiological Society, 1979, pp. 61-112.

[61] D. F. Scollan, A. Holmes, R. Winslow, J. Forder, “Histological validation of myocardial microstructure obtained from diffusion tensor magnetic resonance imaging,” *Am. J. Physiol.*, vol. 275, pp. H2308-H2318, 1998.

[62] E. Hsu, A. Muzikant, S. Matulevicius, R. Penland, C. Henriquez, “Magnetic resonance

myocardial fiber-orientation mapping with direct histological correlation," *Am. J. Physiol.*, vol. 274, pp. H1627-H1634, 1998.

[63] A. D. McCulloch, B. H. Smaill, P. J. Hunter, "Regional left ventricular epicardial deformation in the passive dog heart, *Circ. Res.*, vol. 64, pp. 721-733, 1989.

[64] F. J. Villarreal, L. K. Waldman, W. Y. W. Lew, "A technique for measuring regional two-dimensional finite strains in the canine left ventricle," *Cir. Res.*, vol. 62, pp. 711-721, 1988.

[65] L. K. Waldman, D. Nosan, F. J. Villarreal, J. W. Covell, "Relation between transmural deformation an local myofiber direction in canine left ventricle," *Circ. Res.*, vol. 63, pp. 550-562, 1988.

[66] J. A. Weiss, B. N. Maker, S. Govindjee, "Finite element implementation of incompressible, transversely isotropic hyperelasticity," *Comp. Meths. In Appl. Mechs. And Eng.,* vol. 135, pp. 107-128, 1996.

[67] J. A. C. Martins, E. B. Pires, R. Salvado, P. B. Dinis, "A numerical model of passive and active behavior of skeletal muscles," *Comput. Methods Appl. Mech. Engrg.*, vol. 151, pp. 419-433, 1998.

[68] F. J. Wackers, P. Maniawski, A. J. Sinusas, "Evaluation of left ventricular regional wall function by ECG-gated technetium-99m-sestamibi imaging," in *Nuclear Cardiology – State of the Art and Future Directions*, B. L. Zaret, G. A. Beller, eds., Mosby-Year Book, Inc., St. Louis, MO, pp. 201-208, 1993.

[69] K. P. Gallagher, Matsuzaki, G. Osakada, W. S. Kemper, J. Ross, Jr., "Effect of exercise on the relationship between myocardial blood flow and systolic wall thickening in dogs with acute coronary stenosis," *Circ. Res*., vol. 52, pp. 716-729, 1983.

[70] G. Stroink, W. Moshage, S. Achenbach, "Cardiomagnetism," in *Magnetism in Medicine: A Handbook*, W. Andra, H. Nowak, eds., Wiley-VCH, New York, 1998. pp. 136-189.

[71] L. L. Baker, *et al.*, "Recent advances in MR imaging/spectroscopy of cerebral ischemia,"

AJR Am. J. Roentgenol., vol. 156, pp. 1133-1143, 1991.

[72] S. Warach, *et al.*, "Fast magnetic resonance diffusion-weighted imaging of acute human stroke {published erratum appears in *Neurology*, vol. 42, p. 2192, 1992] *Neurology*, vol. 42, pp. 1717-1723, 1992.

[73] D. Chien, *et al.,* "MR diffusion imaging of cerebral infarction in humans," *AJNR Am. Neuroradiol.*, vol. 13, pp. 1097-1102; discussion pp. 1103-1105, 1992.

[74] D. Le Bihan, *et al.,* "Diffusion MR imaging: Clinical applications," *AJR Am. J. Roentgenol.*, vol. 159, pp. 591-599, 1992.

[75] S. Peled, *et al.,* "Magnetic resonace imaging shows orientation and asymmetry of white matter fiber tracts," *Brain Res.,* vol. 780, pp. 27-33, 1998.

[76] N. Makris, *et al.,* "Morphometry of *in vivo* human white matter association pathways with diffusion-weighted magnetic resonance imaging," *Ann. Neurol.,* vol. 42, pp. 951-962, 1997.

[77] T. E. Conturo, *et al.,* "Tracking neuronal fiber pathways in the living human brain," *Proc. Natl. Acad. Sci. US*, vol. 96, pp. 10422-10427, 1999.

[78] D. J. Werring, *et al.,* "A direct demonstration of both structure and function in the visual system: Combining diffusion tensor imaging with functional magnetic resonance imaging," *Neuroimage*, vol. 9, pp. 352-361, 1999.

[79] S. L. Florence, H. B. Taub, J. H. Kaas, "Large-scale sprouting of cortical connections after peripheral injury in adult macaque monkeys," *Science*, vol. 282, pp. 1117-1121, 1998.

[80] E. A. Zerhouni, D. M. Parish, W. J. Rogers, A. Yang, E. P. Shapiro, "Human heart: Tagging with MR imaging – A method for noninvasive assessment of myocardial motion," *Radiology*, vol. 169, pp. 59-63, 1988.

[81] L. Axel, L. Dougherty, "MR imaging of motion with spatial modulation of

magnetization," *Radiology*, vol. 171, pp. 841-845, 1989.

[82] N. J. Pelc, R. J. Herfkens, A. Shimakawa, D. R. Enzmann, "Phase contrast cine magnetic resonance imaging [review]," *Magn. Reson. Q.*, vol. 7, pp. 229-254, 1991.

[83] E. R. McVeigh, E. A. Zerhouni, "Non-invasive measurement of transmural gradients in myocardial strain with magnetic resonance imaging," *Radiology*, vol. 180, pp. 677-683, 1991.

[84] E. R. McVeigh, "MRI of myocardial function: Motion tracking technique," *Magn. Reson. Imag.*, vol. 14, pp. 137-150, 1996.

[85] S. S. Orlov, "Theory of three-dimensional reconstruction: I. Conditions of a complete set of projections," *Sov. Phys. Crystaalogr.* 20:312-314, 1975.

Figure 1. Geometry illustrating directional Radon projections. The directional Radon projection of the tensor field $T(\underline{x})$ is denoted as $r^{\theta\alpha}(s;\underline{\theta})$ for the planar integral of the scalar function $\underline{\theta}^T T(\underline{x})\underline{\alpha}$ over the plane perpendicular to $\underline{\theta}$ and at a distance s from the origin. Note that $\underline{\theta}$, $\underline{\alpha}$, and $\underline{\beta}$ are the orthogonal vectors given in (6)-(8).

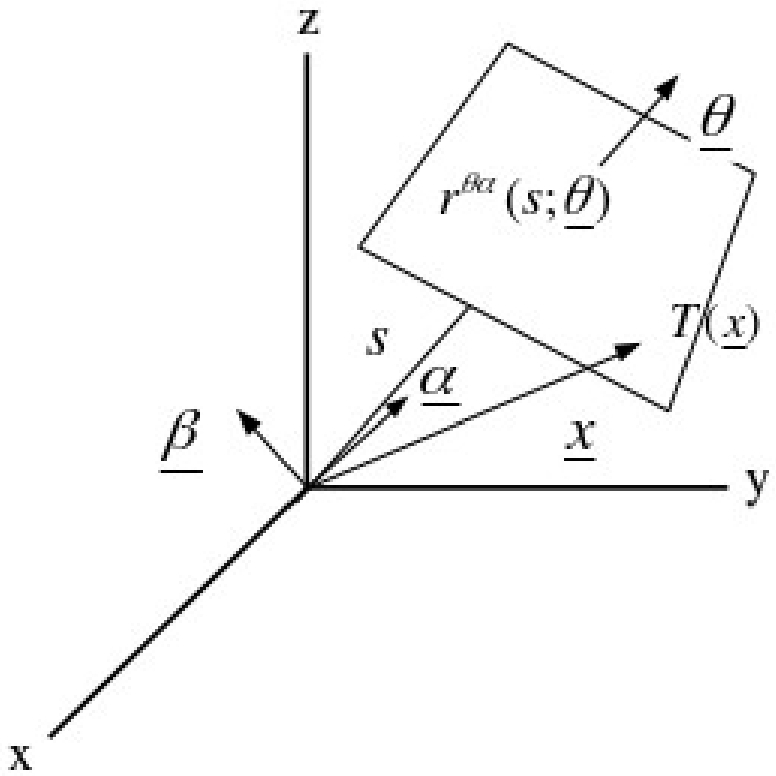

Figure 2. Geometry illustrating directional X-ray projections. The directional X-ray projection of the tensor field $T(\underline{x})$ is denoted as $p^{\theta\alpha}(\underline{s};\underline{\theta})$ for the line integral of the scalar function $\underline{\theta}^T T(\underline{x})\underline{\alpha}$ parallel to $\underline{\theta}$ and at a position $\underline{s}$ in the uv -plane. Note that the origin of the uv -plane is the same as the origin of the xyz -plane.